Chapter 2
Fundamental Processes in Fluid Motion

It has been stated in *Preface* of this book that the physics of vortical flows can be fully understood only if the subject is put on a broad background about the splitting and coupling of different fundamental dynamic processes in fluid motion. The concept of process splitting has been repeatedly touched upon in Chap. 1, both kinematically and dynamically, when we discuss dilatation and vorticity, decomposition of velocity gradient, strain-rate tensor, dynamic constitutive relation and stress tensor, the Navier-Stokes equations, and dominant dimensionless parameters. Accordingly, the stress force is split into normal and tangent components, and velocity boundary condition is split to normal no-through and tangent no-slip conditions. In this chapter we present a systematic theory on this subject, starting from a physical explanation of fundamental processes in fluid motion, in non-mathematical language.

2.1 Preliminary Observations

Conceive a piston suddenly put in slight motion at $t = 0$, in a one-dimensional pipe flow which was originally at rest. Then the fluid at one side of the piston is compressed with higher pressure and density, while that at the other side is rarefied with lower pressure and density. If the piston suddenly stops after a short time, opposite processes will occur. Like an elastic body, the fluid cannot be indefinitely compressed and has a *normal elasticity* (for which a more common term is *compressibility*) to resist the compressing, which causes a propagating wave in which the fluid is alternatively compressed and expanded. This is *longitudinal* acoustic wave or sound wave. Owing to the involvement of thermodynamics, many weak compressing waves may squeeze together to form a stronger wave and even an almost discontinuity of fluid properties across the wavefront, namely a shock wave. In this compressing process all fluid elements are acted by a pressure force (modified by a viscous normal stress) like many micro-pistons. Compressing process is one of the basic forms of existence of the fluid motion.

J.-Z. Wu et al., *Vortical Flows*, DOI 10.1007/978-3-662-47061-9_2

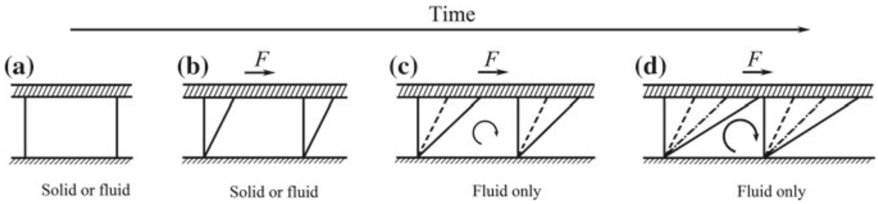

Fig. 2.1 Shearing process between parallel plates and driven by upper plate. **a** and **b** Finite deformation of elastic body. **a**–**d** Indefinitely deforming of fluid and formation of shear layer, in which vorticity is enhancing as time goes on. Based on Pritchard (2011)

Conceive now a viscous fluid and an elastic solid test substance between two parallel plates, and let the lower plate be stationary and upper plate start to move suddenly in its plane. If the test substance is an elastic solid, the imposed shear force deforms slightly the solid and causes a shear stress proportional to the displacement that stops the motion (Fig. 2.1a, b). In sharp contrast, if the test substance is a viscous fluid, although the shear force exerted by upper plate also drives a thin adjacent fluid layer to move which in turn drives the next thin fluid layer and so on, the fluid has no shear elasticity at all but just responses the force by indefinite deformation till the force is balanced by a shear stress proportional to the normal gradient of velocity (Fig. 2.1a through d), in which fluid elements have to rotate and thereby gain *vorticity*. This flow pattern exemplifies another fundamental process or the basic form of existence in fluid motion, known as *transverse process* or *shearing process*. Any fluid more or less has a shear viscosity, and thus the shearing is also a universal process in fluid motion.

The lack of shear elasticity in fluid is closely related to its *fluidity*. When an aircraft flies in the air or a fish swims through the water, it not only separates the surrounding fluid, which moves away from its path and forms a variable pressure distribution on the surface of aircraft (or fish); but also, it “rubs” the fluid to form a *shear layer* attached to its surface. A shear layer is the primary structure in vortical flows, also known as *layer-like vortex* (this is a more general use of the term “vortex”). If the wall has a downstream end, the attached shear layer sheds off to become a free shear layer. A sufficiently thin free shear layer may automatically roll into a concentrated *axial vortex*, which is the secondary (and stronger) structures of vortical flows. Therefore, vorticity and vortices are the major product of the shearing process and exist only in fluids. In this regards the very insightful assertion of Shi-Jia Lu, the only female disciple of Ludwig Prandtl, that the present authors have cited in many occasions, deserves to be cited again:

The essence of fluid is vortices. A fluid cannot stand rubbing; once you rub it there appear vortices.

Fluid dynamics would still be simple if the compressing and shearing processes could always evolve independent of each other. This is however not true: generically they are coupled as sketched in Fig. 2.2. For example, owing to the viscosity, in the pipe-piston system the fluid elements near the pipe wall must be rubbed by tangent

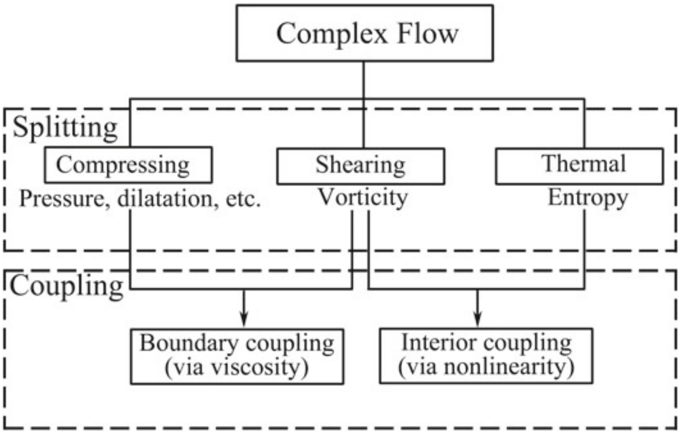

Fig. 2.2 Schematic diagram of decomposition and coupling of fundamental dynamic processes in a generic complex flow

pressure gradient, the longitudinal sound wave or shock wave, and the flow cannot be strictly one-dimensional and irrotational. On the other hand, the motion and interaction of vortices must alter the surrounding pressure distribution, including producing sound. Note that even in incompressible flow model decoupled from thermodynamics, the compressing process still exists but is solely represented by a *mechanical pressure*, of which the key role in vortical flow is to generate new vorticity at a wall via its tangent gradient. The generated vorticity is soon diffused into the interior of fluid. This event is a major product of boundary coupling between shearing and compressing.

The theory on the splitting and coupling of these three fundamental processes may serve as a sharp scalpel to investigate the extremely rich and complex flow patterns seen in nature and technology. It also guides one to best understand the inherent connections and distinctions of various disciplines of fluid dynamics.

In Sect. 2.2 we introduce the most powerful mathematic tool of vector decomposition, the *Helmholtz decomposition*, and apply it to the momentum balance to derive the dynamic equations for vorticity and dilatation. Section 2.3 addresses the coupling of the processes, both inside the flow field and at boundary. In Sect. 2.4 we consider far-field dynamic asymptotics of vorticity and dilatation in unbounded domain and thereby derive the velocity far-field behavior. Sections 2.5 and 2.6 introduce two widely used decoupled and minimally coupled model flows, the inviscid compressible flow and viscous incompressible flow, respectively. The latter will be the major model in our study of vortical flows in the rest of the book.

2.2 Intrinsic Decomposition of Fundamental Processes

2.2.1 Helmholtz Decomposition

The *Helmholtz decomposition*[1] states that for any continuous vector field $\boldsymbol{f}$ in a bounded or unbounded domain there must exist scalar field ϕ and solenoidal vector field $\boldsymbol{A}$, known as the scalar and vector *Helmholtz potentials* of $\boldsymbol{f}$, respectively, such that $\boldsymbol{f}$ can be globally decomposed to

$$\boldsymbol{f} = \nabla\phi + \nabla \times \boldsymbol{A}, \quad \nabla \cdot \boldsymbol{A} = 0. \tag{2.2.1}$$

For a given vector field $\boldsymbol{f}$, ϕ and $\boldsymbol{A}$ can be obtained by solving Poisson equations derived from (2.2.1):

$$\nabla^2\phi = \nabla \cdot \boldsymbol{f}, \quad \nabla^2\boldsymbol{A} = -\nabla \times \boldsymbol{f}. \tag{2.2.2}$$

For a full discussion of this decomposition see Appendix A.3.2. For example, the decomposition (1.1.17) of $\nabla^2\boldsymbol{u}$,

$$\nabla^2\boldsymbol{u} = \nabla(\nabla \cdot \boldsymbol{u}) - \nabla \times (\nabla \times \boldsymbol{u}) = \nabla\vartheta - \nabla \times \boldsymbol{\omega}, \tag{2.2.3}$$

is a kinematic Helmholtz decomposition, indicating that the vector field $\nabla^2\boldsymbol{u}$ consists of (or can be intrinsically split into) the gradient of scalar ϑ, which is a curl-free vector, and the curl of vector $\boldsymbol{\omega}$, which is a solenoidal or divergence-free vector.

Then, let $\boldsymbol{a} = D\boldsymbol{u}/Dt$, the Navier-Stokes equation in the form of (1.2.31b) for constant μ also appears as a *dynamic* Helmholtz decomposition of the total body force (inertial force $-\rho\boldsymbol{a}$ plus external body force $\rho\boldsymbol{f}$)[2]:

$$\rho(\boldsymbol{f} - \boldsymbol{a}) = \nabla\Pi + \nabla \times (\mu\boldsymbol{\omega}), \tag{2.2.4}$$

where $\Pi = p - \mu_\theta\vartheta$ and $\mu\boldsymbol{\omega}$ are the scalar and vector Helmholtz potentials of the total body force, respectively. Some of the underlying physics of this decomposition has been discussed in Chap. 1. Its exact existence lies in the fact that the Helmholtz decomposition is a linear operation and so is the constitutive relations of Newtonian fluid. According to our terminology defined in Sect. 1.1.2, the fields of ϑ and Π are longitudinal and that of $\boldsymbol{\omega}$ is transverse.

The Helmholtz decomposition can also be applied to velocity field itself, say

$$\boldsymbol{u} = \nabla\phi + \nabla \times \boldsymbol{\psi}, \quad \nabla \cdot \boldsymbol{\psi} = 0. \tag{2.2.5}$$

[1] According to Truesdell (1954), this decomposition should bear the name of G. G. Stokes who first introduced it in 1851. Here we just follow the convention.

[2] The notation $\boldsymbol{f}$ here should not be confused with the general vector field introduced in (2.2.1). This form of the N-S equation was first observed by Poisson in 1829 and re-emphasized by Truesdell (1954).

A difference between (2.2.3) or (2.2.4) and (2.2.5) is worth noticing. The first two are *natural* because their potentials themselves are physical fields. By contrast, (2.2.5) is a somewhat artificial treatment where the potentials are auxiliary functions and have to be calculated by solving (2.2.2). Nevertheless, to this end a comparison of (2.2.1) and (2.2.3) can slightly simplify our task. We just introduce an auxiliary vector field $\boldsymbol{F}$ such that $\boldsymbol{F}$ satisfies a single vector Poisson equation with source $\boldsymbol{u}$:

$$\boldsymbol{u} = \nabla^2 \boldsymbol{F} = \nabla(\nabla \cdot \boldsymbol{F}) - \nabla \times (\nabla \times \boldsymbol{F}) = \nabla\phi + \nabla \times \boldsymbol{\psi}.$$

Thus, $\boldsymbol{F}$ can be solved for given $\boldsymbol{u}$ under proper boundary condition, and then $(\phi, \boldsymbol{\psi})$ can be obtained from $\nabla \cdot \boldsymbol{F}$ and $\nabla \times \boldsymbol{F}$. The procedure is given in Appendix A.3.2. Then one may further proceed to finding $\boldsymbol{u}$ for given ϑ and $\boldsymbol{\omega}$. This is the inversion of (1.1.12), as the equations therein are viewed as differential equations for $\boldsymbol{u}$ with given $(\vartheta, \boldsymbol{\omega})$ field. The result is the famous Biot-Savart formula to be discussed in Chap. 3.

In unbounded domain, if $\boldsymbol{f}$ approaches zero fast enough as $|\boldsymbol{x}| \to \infty$, the solutions of (2.2.2) exist and are unique, and hence so are the Helmholtz potentials; but in a bounded domain this is not the case without prescribing boundary conditions. In this regard, we have the **Helmholtz-Hodge theorem** proved in Sect. A.3.2:

A finite and continuous vector field $\boldsymbol{f}(\boldsymbol{x})$ in a bounded domain V can always be uniquely split into a longitudinal part $\nabla\phi$ and a transverse part $\mathbf{f}_\perp$, where $\nabla \cdot \mathbf{f}_\perp = 0$ and

$$\boldsymbol{n} \cdot \boldsymbol{f}_\perp = 0 \quad \text{or} \quad \frac{\partial \phi}{\partial n} = \boldsymbol{n} \cdot \boldsymbol{f} \quad \text{at } \partial V. \tag{2.2.6}$$

In this case $\mathbf{f}_\perp$ and $\nabla\phi$ are functionally orthogonal in V in the sense that

$$\int_V \nabla\phi \cdot \boldsymbol{f}_\perp dV = 0. \tag{2.2.7}$$

Similar to the geometric orthogonality, being functional orthogonality implies physical decoupling of these two vector fields. Note that in (2.2.1) one can further separate a harmonic function ζ from scalar ϕ with $\nabla^2\zeta = 0$, such that $\nabla\zeta$ is also functionally orthogonal to both $\nabla\phi$ and $\boldsymbol{f}_\perp$. Thus, strictly, $\boldsymbol{f}$ has a *triple orthogonal decomposition*. The harmonic part is necessary for satisfying boundary conditions and thereby influences both.

Whether the Helmholtz-Hodge theorem can be applied to a specific vector field in V depends critically on the physical behavior of this field. For example, for an incompressible flow over a stationary body, the no-through condition at the body surface implies that the velocity $\boldsymbol{u}$ is a transverse vector and satisfies (2.2.6). But in dynamic decomposition (2.2.4) the solenoidal part $\nabla \times \boldsymbol{\omega}$ is generally not parallel to the boundary, since $\boldsymbol{n} \cdot (\nabla \times \boldsymbol{\omega}) = (\boldsymbol{n} \times \nabla) \cdot \boldsymbol{\omega}$ can be nonzero in viscous flow as long as $\boldsymbol{\omega}$ varies along the boundary. Rather, the full adherence condition stated in Sect. 1.3.1 implies that there will appear a pair of *boundary coupling relations* between two Helmholtz potentials. The boundary dynamic coupling of Π and $\mu\boldsymbol{\omega}$ will be extensively discussed latter in Sects. 2.3.2 and 3.4.4, which implies the violation of the orthogonality condition (2.2.7). Consequently, Π and $\mu\boldsymbol{\omega}$ are globally coupled.

2.2.2 Dynamic Equations for Vorticity and Dilatation

In this subsection we seek a thorough natural decomposition of the momentum equation, which enables deriving the dynamic equations for vorticity and dilatation. While the dynamic Helmholtz decomposition (2.2.4) is already a very informative formulation of the momentum balance, this equation alone is insufficient to fully understand the properties of fundamental processes and their coupling mechanisms. It is still necessary to go through all equations in (1.2.31). Besides, (2.2.4) is for fluid elements per unit volume, where the inertial force $-\rho\boldsymbol{a} = -\rho D\boldsymbol{u}/Dt$ is taken as a whole; but in the field description the acceleration itself should be further decomposed, and vorticity and dilatation are defined for unit mass. Therefore, we should consider the momentum equation per unit mass:

$$\boldsymbol{a} = -\frac{1}{\rho}\nabla p + \boldsymbol{\eta} = -\nabla h + T\nabla s + \boldsymbol{\eta}, \tag{2.2.8a}$$

where we have set external body force $\boldsymbol{f} = \mathbf{0}$ for simplicity. The replacement of pressure by enthalpy via (1.2.26) makes the entropy gradient appear explicitly, which is expected to be the root of the coupling of dynamic processes and irreversible thermodynamics. The vector $\boldsymbol{\eta}$ represents all viscous effects, which by (1.2.18) reads

$$\boldsymbol{\eta} \equiv \frac{1}{\rho}\nabla\cdot\mathbf{V} = \nu_\theta\nabla\vartheta - \nu\nabla\times\boldsymbol{\omega}, \tag{2.2.8b}$$

where the shearing and longitudinal kinematic viscosities

$$\nu = \frac{\mu}{\rho}, \quad \nu_\theta = \frac{\mu_\theta}{\rho} \tag{2.2.9}$$

must be variable for compressible flow. In this case, unlike (2.2.4), on both sides of (2.2.8a) no term except ∇h can be naturally decomposed. We have to treat them one by one.

First, we re-express the acceleration by (1.1.36),

$$\boldsymbol{a} = \frac{\partial\boldsymbol{u}}{\partial t} + \boldsymbol{\omega}\times\boldsymbol{u} + \nabla\left(\frac{1}{2}q^2\right) \tag{2.2.10}$$

to display a natural longitudinal term. Thus (2.2.8a) becomes

$$\frac{\partial\boldsymbol{u}}{\partial t} + \boldsymbol{\omega}\times\boldsymbol{u} = -\nabla H + T\nabla s + \boldsymbol{\eta}, \quad H = h + \frac{1}{2}q^2, \tag{2.2.11}$$

known as the *Crocco-Vazsonyi equation*, where H is the total enthalpy.

Next, let ν_0 and $\nu_{\theta 0}$ be constant reference values of ν and ν_θ, respectively, we write

$$\nu = \frac{\mu}{\rho} = \nu_0(1+\tilde{\nu}'), \quad \nu_\theta = \frac{\mu_\theta}{\rho} = \nu_{\theta 0}(1+\tilde{\nu}'_\theta), \tag{2.2.12a}$$

such that

$$\boldsymbol{\eta} = \nabla(\nu_{\theta 0}\vartheta) - \nabla \times (\nu_0 \boldsymbol{\omega}) + \boldsymbol{\eta}', \tag{2.2.12b}$$
$$\boldsymbol{\eta}' = \nu_{\theta 0}\tilde{\nu}'_\theta \nabla\vartheta - \nu_0 \tilde{\nu}' \nabla \times \boldsymbol{\omega}. \tag{2.2.12c}$$

Since $\boldsymbol{\eta}'$ is generically of smaller order unless $\tilde{\nu}'$ and $\tilde{\nu}'_\theta$ have exceptionally strong variation, we ignore it in the following discussion.

With these preparations, (2.2.11) is cast to

$$\frac{\partial \boldsymbol{u}}{\partial t} + \nabla(H - \nu_{\theta 0}\vartheta) + \nabla \times (\nu_0 \boldsymbol{\omega}) = -\boldsymbol{L}, \tag{2.2.13a}$$

where

$$\boldsymbol{L} \equiv \boldsymbol{\omega} \times \boldsymbol{u} - T\nabla s \tag{2.2.13b}$$

is genuinely nonlinear that has both divergence and curl. We call $\boldsymbol{L}$ the *generalized Lamb vector*.

Equation (2.2.13a) exhibits as much the "natural" Helmholtz decomposition as we can reach. We now substitute the velocity decomposition (2.2.5) into (2.2.13a) as the only "artificial" element of our decomposition:

$$\nabla\left(\frac{\partial \phi}{\partial t} + H - \nu_{\theta 0}\vartheta\right) + \nabla \times \left(\frac{\partial \boldsymbol{\psi}}{\partial t} + \nu_0 \boldsymbol{\omega}\right) = -\boldsymbol{L}. \tag{2.2.14}$$

Naturally, to study each of shearing and compressing processes as well as their coupling, we can take the curl and divergence of (2.2.14).[3] On the one hand, its curl yields

$$\frac{\partial \boldsymbol{\omega}}{\partial t} - \nu_0 \nabla^2 \boldsymbol{\omega} = -\nabla \times \boldsymbol{L}, \quad \boldsymbol{\omega} = -\nabla^2 \boldsymbol{\psi}, \tag{2.2.15}$$

which is the basic equation of vorticity dynamics for the shearing process and will be discussed extensively throughout this book. On the other hand, the divergence of (2.2.14) leads to an equation for the compressing process:

$$\frac{\partial \vartheta}{\partial t} + \nabla^2(H - \nu_{\theta 0}\vartheta) = -\nabla \cdot \boldsymbol{L}, \quad \vartheta = \nabla^2 \phi, \tag{2.2.16}$$

[3] Equivalently but without raising the order of equation, one may project (2.2.14) onto a solenoidal vector space to remove its longitudinal part, see, e.g. Chorin and Marsden (1992).

which is however merely an intermediate product due to the involvement of another longitudinal variable H. In fact, for compressible flow with nonzero ϑ or Mach number, the continuity Equation (1.2.31a) and energy equation, say (1.2.31c), have to be combined with (2.2.16) to jointly describe both compressing and thermodynamic processes. This procedure has been conducted by Mao et al. (2011). After a lengthy algebra, they obtained a general viscous dilatation equation for polytropic gases:

$$\frac{\partial^2 \vartheta}{\partial t^2} - \nabla^2 \left[\left(a^2 + \nu_\theta \frac{D}{Dt} \right) \vartheta \right] = Q_\theta, \quad \text{with} \tag{2.2.17a}$$

$$\begin{aligned} Q_\theta &= -\nabla^2 \left[\left(\frac{D}{Dt} + \frac{\partial}{\partial t} \right) \left(\frac{1}{2} q^2 \right) \right] - \left(\frac{\partial}{\partial t} + \nu \nabla^2 \right) \nabla \cdot (\boldsymbol{\omega} \times \boldsymbol{u}) - \nu \nabla^2 \omega^2 \\ &+ \frac{1}{(\gamma - 1) c_v} \nabla \cdot \left[\frac{1}{\gamma} \frac{\partial}{\partial t} (a^2 \nabla s) + \frac{1}{\gamma} \nabla (a^2 \boldsymbol{u} \cdot \nabla s) - \nabla \left(a^2 \frac{Ds}{Dt} \right) \right]. \end{aligned} \tag{2.2.17b}$$

The basic structure of this complicated equation is seen from the left-hand side of (2.2.17a). It is a *parabolic* equation for viscous longitudinal wave, of one order higher than (2.2.15) and (2.2.16) due to the removal of H from the latter. The sound speed a is to be calculated from the energy equation (recall $a^2 = (\gamma - 1)h$). When $\nu_\theta = 0$, (2.2.17) degenerates to an inhomogeneous *hyperbolic* wave equation as it should. Q_θ collects nonlinear terms from the Lamb vector, variation of kinetic energy, vorticity, and entropy, whose physical roles will be classified in the next subsection.

Equations (2.2.15) and (2.2.17) may be viewed as a pair of general coupled dynamic equations for the shearing and compressing equations. They are both of parabolic type, but with distinct physical-mathematical properties reflecting the very different characteristics of flow structures in shearing and compressing processes. When the two processes coexist, one should carefully observe the respective distributions and motions of these structures and thereby trace their physical origins.

To exemplify the complex coexistence of the two processes, Fig. 2.3 shows one of a sequence of photos as a vertical plane shock strikes a finite 25° wedge. As the shock wave passes the wedge base, the flow separates to form thin vortex layers that roll up into discrete vortices (these mechanisms will be discussed in later chapters). Further interaction produces increasingly complex pattern of shock waves, vortex layers, and vortices [for the whole sequence see Van Dyke (1982)]. Figure 2.4 shows a fighter plane flying at $M_\infty \simeq 1$. At the wing's upper surface the flow is supersonic and full of expansion waves made visible by moisture condensation, which coexists with wingtip vortices.

Figure 2.5 is a slice of the $(\boldsymbol{\omega}, \vartheta)$ distribution for a compressible isotropic turbulence at a large Reynolds number and turbulent Mach number $M_t = u'/\langle a \rangle = 1.03$, where u' is the root-mean-square (rms) turbulence velocity and $\langle a \rangle$ is the mean speed of sound. While the vorticity field exhibits intermittent filament-like structures, the dilatation field is highly peaked at some sheet-like shock waves with extremely

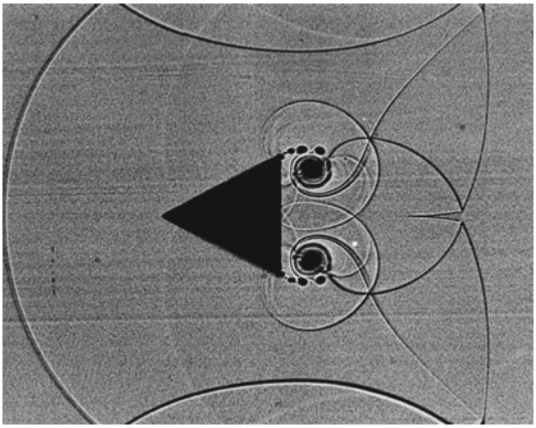

Fig. 2.3 Shock-vortex interaction during the diffraction of a shock wave by a finite wedge. From Van Dyke (1982), Fig. 241

Fig. 2.4 Coexistence of wingtip vortices and supersonic waves around a fighter flying at nearly sound speed. Courtesy of http://www.sky-flash.com/EJ.v.Koningsveld

strong $\vartheta < 0$ called shocklets (in their near neighborhood the vortical structures may become sheet-like as well). Statistically, Wang et al. (2012, 2013) have observed that the vortical structures obey the same law as those in incompressible flow, while the dilatation structures obey a law similar to one-dimensional shocklets (recall that compressing process exists for one- to three-dimensional flows).

2.3 Coupling and Splitting of Fundamental Processes

The Helmholtz decomposition is a linear operator, but the Navier-Stokes equation contains various nonlinear terms that cause process coupling inside the fluid. Besides, a linear and viscous coupling occurs at boundary due to no-slip condition. Both coupling mechanisms are discussed in this section.

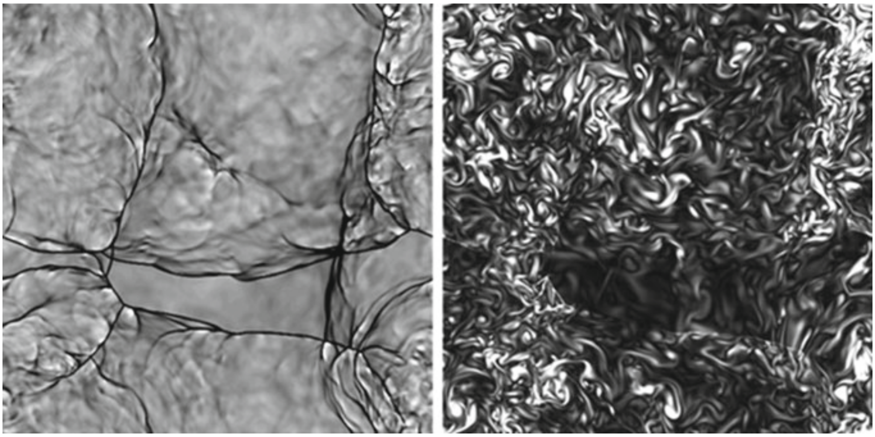

Fig. 2.5 The distribution of dilatation (*left*) and vorticity (*right*) on a slice of a three-dimensional and high Mach-number isotropic turbulence. Direct numerical simulation with grid 512^3 at turbulent Mach number $M_t = 1.03$. Courtesy of Shiyi Chen

2.3.1 Process Nonlinearity and Coupling Inside the Flow

In the interior of the fluid motion the coupling mechanisms of different processes can be identified from the nonlinear terms of (2.2.15) and (2.2.17). To see the respective role of each nonlinear term in each process, we first follow Mao et al. (2011) to consider a pair of coupled nonlinear model equations for functions f and g in a domain $(x, t) \in \mathcal{D}$:

$$f_t + f_x^2 - \epsilon g_x f = 1, \tag{2.3.1a}$$

$$g_t - g g_x - f f_x = 0, \tag{2.3.1b}$$

where subscripts denote partial derivatives. The nonlinear terms in these equations fall into three types:

(1) *Cross generation*: A nonlinear mechanism from motion g (or f) that serves as the inhomogeneous source of another motion f (or g), so that it can *produce* motion f (or g) from nothing. Of this type is $-f f_x$ in (2.3.1b), since for example if $g = 0$ at $t = 0$ then after a small time interval δ there will be

$$g = \int_0^\delta f f_x dt + O(\delta^2).$$

(2) *Cross modulation*: A nonlinear mechanism in the evolution of motion f (or g) by which motion g (or f) modulates the evolution of existing f (or g) but not creates it from nothing. Of this type is $-\epsilon g_x f$ in (2.3.1a).

(3) *Self-nonlinearity*: A nonlinear mechanism that takes place within each motion. Of this type are f_x^2 in (2.3.1a) and $-gg_x$ in (2.3.1b). For example, if ϵ is negligibly small in a subdomain $\mathcal{D}_1$, there will be

$$f_t + f_x^2 = 1 \quad \text{in} \quad \mathcal{D}_1.$$

This self-nonlinearity will affect the coupling with process g indirectly through types (1) and (2).

Let us now revisit (2.2.15) and (2.2.17). First, of all nonlinear terms therein, the generalized Lamb vector $\boldsymbol{L} = \boldsymbol{\omega} \times \boldsymbol{u} - T\nabla s$ stands at the crossroad of the two dynamic processes. It appears in both equations.[4] This vector is the most commonly encountered mechanism of the compressing-shearing coupling in the interior of a flow field. More specifically, write $\boldsymbol{u} = \boldsymbol{v} + \nabla\phi$ such that $\boldsymbol{v}$ is the transverse part (including the harmonic part induced by the vorticity field, so that ϕ always represents the compressible potential flow induced by ϑ), the Lamb vector is split into $\boldsymbol{\omega} \times \boldsymbol{v}$ and $\boldsymbol{\omega} \times \nabla\phi$. Since $\boldsymbol{\omega} = \nabla \times \boldsymbol{v}$, the former is purely transverse; but the latter implies cross modulation.

Next, for clarity, denote terms for self nonlinearity, cross generation, and cross modulation by SN, CG, and CM, respectively. Then in the shearing equation (2.2.15), $\nabla \times \boldsymbol{L}$ is the *only* nonlinear term and can be expanded to

$$\nabla \times \boldsymbol{L} = \underbrace{\nabla \times (\boldsymbol{\omega} \times \boldsymbol{v})}_{SN} + \underbrace{\nabla \times (\boldsymbol{\omega} \times \nabla\phi)}_{CM} - \underbrace{\nabla T \times \nabla s}_{CG}. \tag{2.3.2}$$

Here, the first term is a self nonlinearity of the shearing process, which will be discussed in detail later; the third term is an external source from entropy process that appears in baroclinic flow; and the second term exhibits how a compressing process modulates an existing shearing process which, by denoting $\boldsymbol{u}_\phi = \nabla\phi$, can be written as

$$\nabla \times (\boldsymbol{\omega} \times \boldsymbol{u}_\phi) = \boldsymbol{u}_\phi \cdot \nabla\boldsymbol{\omega} - \boldsymbol{\omega} \cdot \nabla\boldsymbol{u}_\phi + \vartheta\boldsymbol{\omega}.$$

In contrast, in compressing process governed by (2.2.17), we see that physical sources of the ϑ-wave are contained in the three explicitly time-dependent terms on the right-hand side: the divergence of Lamb vector,[5] the kinetic energy, and the entropy gradient, of which the first two are major nonlinear terms and we split them to

$$\nabla \cdot (\boldsymbol{\omega} \times \boldsymbol{u}) = \underbrace{\nabla \cdot (\boldsymbol{\omega} \times \boldsymbol{v})}_{CG} + \underbrace{(\nabla \times \boldsymbol{\omega}) \cdot \nabla\phi}_{CM}, \tag{2.3.3a}$$

$$\frac{1}{2}\nabla^2|\boldsymbol{u}|^2 = \underbrace{\frac{1}{2}\nabla^2|\boldsymbol{v}|^2}_{CG} + \underbrace{\frac{1}{2}\nabla^2|\nabla\phi|^2}_{SN} + \underbrace{\nabla^2(\boldsymbol{v} \cdot \nabla\phi)}_{CM}. \tag{2.3.3b}$$

[4]In Chap. 3 we shall see some special types of flows where the Lamb-vector effect disappears completely or partly, although both $\boldsymbol{\omega}$ and $\boldsymbol{u}$ are nonzero.

[5]The longitudinal waves produced by this mechanism is called *vortex sound*.

Except a self-nonlinearity $\nabla^2(|\nabla\phi|^2/2)$, there are two external sources, $\nabla\cdot(\boldsymbol{\omega}\times\boldsymbol{v}-T\nabla s)$ and $\nabla(|\boldsymbol{v}|^2/2)$, and two cross-modulation mechanisms, $\nabla^2(\boldsymbol{v}\cdot\nabla\phi)$ and $(\nabla\times\boldsymbol{\omega})\cdot\nabla\phi$, where the former represents the convection of ϕ by the shearing velocity $\boldsymbol{v}$, as is evident from (2.2.16) in which

$$\partial_t\vartheta+\nabla^2(\boldsymbol{v}\cdot\nabla\phi)=\nabla^2[(\partial_t+\boldsymbol{v}\cdot\nabla)\phi].$$

Note that *the shearing process can be a source of compressing process, but not vise versa.*[6]

2.3.2 Process Linear Coupling on Boundaries

The compressing and shearing processes are also coupled on flow boundary ∂V but by a different mechanism. To see this we first notice that (2.2.15) and (2.2.16) are one order higher than the original N-S equation (2.2.4), indicating that their boundary conditions are not only the velocity adherence (1.3.2) but also one-order higher, the acceleration adherence (1.3.3), i.e., $[\![\boldsymbol{a}]\!]=\boldsymbol{0}$, for otherwise there may appear spurious solutions due to the raising of the order. Dynamically, this requires applying the N-S equation itself to ∂V.

Then, because (1.3.3) takes $\boldsymbol{a}$ as a whole on the material boundary, it is convenient to start from the Navier-Stokes equation (2.2.4) rather than (2.2.13a). As observed in Sect. 2.2.1, the Helmholtz-Hodge theorem is not applicable; there appears a boundary coupling mechanism between Π and $\mu\boldsymbol{\omega}$. Below we illustrate the physical implication of this coupling by considering a high-Re steady and two-dimensional flow over a stationary airfoil C on the (x, y) plane, of which the streamline pattern is sketched in Fig. 2.6.

For this flow (2.2.4) is reduced to

$$\boldsymbol{u}\cdot\nabla\boldsymbol{u}=-\frac{1}{\rho}\nabla p-\nu\nabla\times\boldsymbol{\omega}, \tag{2.3.4}$$

where ρ and ν are constant, and $\boldsymbol{\omega}=\omega\boldsymbol{e}_3$. Let $\boldsymbol{n}$ be the unit normal of any streamline (including the airfoil C), and $\boldsymbol{u}=\boldsymbol{t}q$ be the velocity with $\boldsymbol{t}$ being the unit tangent vector. Assume $\boldsymbol{t}$ moves counterclockwise viewed on the fluid side but clockwise viewed on the body side. Then $(\boldsymbol{n},\boldsymbol{t},\boldsymbol{e}_3)$ form a right-hand orthonormal triad. Denote the arclength of the streamline by s so that

$$\frac{\partial\boldsymbol{t}}{\partial s}=\kappa\boldsymbol{n}, \tag{2.3.5}$$

[6]The above splitting of the nonlinear source terms in (2.2.17) indicates that they still contain some elements of compressing process itself but not expressible by dilatation, unless introducing integral operator.

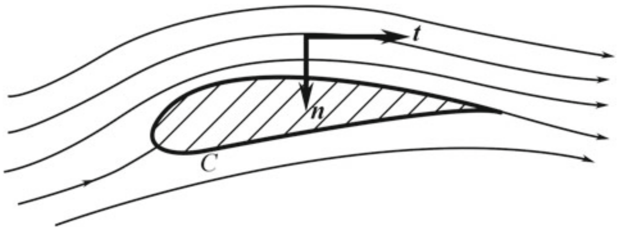

Fig. 2.6 Two-dimensional steady streamlines over an airfoil and intrinsic coordinates

where κ is the curvature of the streamline. Then there is

$$\boldsymbol{u}\cdot\nabla\boldsymbol{u} = q\partial_s q\boldsymbol{t} + \kappa q^2\boldsymbol{n}, \quad -\boldsymbol{t}\cdot(\nabla\times\boldsymbol{\omega}) = \partial_n\omega, \quad -\boldsymbol{n}\cdot(\nabla\times\boldsymbol{\omega}) = -\partial_s\omega.$$

Substituting these into (2.3.4) yields

$$\frac{1}{\rho}\frac{\partial p}{\partial s} = -q\frac{\partial q}{\partial s} + \nu\frac{\partial\omega}{\partial n}, \tag{2.3.6a}$$

$$\frac{1}{\rho}\frac{\partial p}{\partial n} = -\kappa q^2 - \nu\frac{\partial\omega}{\partial s}. \tag{2.3.6b}$$

Obviously, in the effectively inviscid region where $\nu|\nabla\times\boldsymbol{\omega}| \ll 1$, the streamwise pressure gradient is balanced by the streamwise variation of the kinetic energy, while the normal pressure gradient is balanced by the turning of the streamlines if $q \neq 0$ (for a given normal pressure gradient, the smaller q must be associated with sharper turning).

As we move from the effectively inviscid region toward the airfoil C (a special streamline) and finally reach C, however, the momentum-balance mechanism changes dramatically. The no-slip condition requires $q = 0$ there, so by (2.3.6) the gradient of pressure has to be solely balanced by those of vorticity:

$$\frac{1}{\rho}\frac{\partial p}{\partial s} = \nu\frac{\partial\omega}{\partial n}, \tag{2.3.7a}$$

$$\frac{1}{\rho}\frac{\partial p}{\partial n} = -\nu\frac{\partial\omega}{\partial s}. \tag{2.3.7b}$$

This pair of equations represents *a strong viscous and linear coupling of the two fundamental processes at boundaries, and implies a global* $(\boldsymbol{\omega}, p)$ *coupling*.

The most important observation of this boundary coupling is that the vorticity diffusion flux $\nu\partial\omega/\partial n$ at the solid wall as seen in (2.3.7a) is radically different from that inside the fluid as seen in (2.3.6a). In the latter case the vorticity is simply diffused from one side of the streamline to the other side; but since no vorticity exists inside the stationary airfoil, in the former case $\nu\partial\omega/\partial n$ implies that the vorticity is diffused only at the fluid side, either toward or away from the wall. Lighthill (1963) points

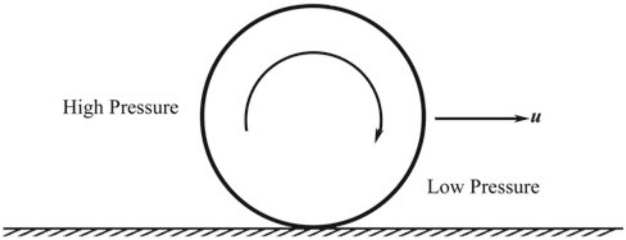

Fig. 2.7 Schematic illustration of vorticity generation by pressure gradient and no-slip condition

out that, this *boundary vorticity flux* measures how much vorticity is created at the wall due to the no-slip condition and sent into the fluid by diffusion in per unit area and unit time. Therefore, (2.3.7a) represents a mechanism that *the tangent pressure gradient at the wall produces vorticity due to adherence.*

To picture this mechanism, Fig. 2.7 shows a small fluid ball right on the wall. Assume at $t = 0$ there suddenly appears a tangent pressure gradient $\partial_s p < 0$, which forces the ball to move right. The ball cannot slide at the wall but only rolls, and hence gains an angular velocity or vorticity ω. Because for $n > 0$ (inside the wall) and $t < 0$ there is $\omega = 0$, the vorticity in the rolling ball must be *newly created* by the joint action of $\partial_s p$ and no-slip condition. The created $\omega < 0$ first occurs in the fluid layer adjacent to the wall and is diffused to the region $n < 0$, with decreasing magnitude at larger distance above the wall. The vorticity will be positive if $\partial_s p > 0$. This mechanism is precisely described by the right-hand side of (2.3.7a), which is a normal vorticity diffusion flux. A general theory of this boundary coupling and vorticity generation will be addressed later in Sect. 3.4.4.

Example 1: Water hammer. Consider a very long water-pipe flow with a valve as sketched in Fig. 2.8. When the valve is being closed, its upstream flow will be stagnated with an increase of pressure p, while the flow downstream will firstly gain a low pressure that propagates at sound speed (the water is slightly compressible) to and is reflected back at the far-downstream open end of the pipe, to become a high-pressure peak that then runs upstream and hits the valve like a hammer. This process happens periodically as the p-wave runs back and forth repeatedly, which may cause severe damage to the valve and nearby hydraulic facilities. Thus, the water-hammer prediction and control are a crucial issue in various hydraulic pipeline systems.

Fig. 2.8 Sketch of water hammer flow

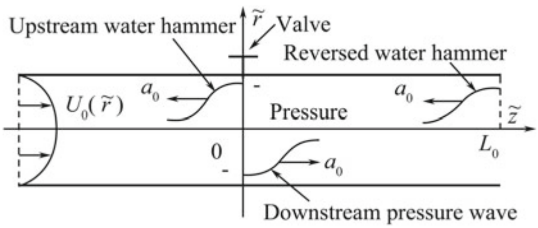

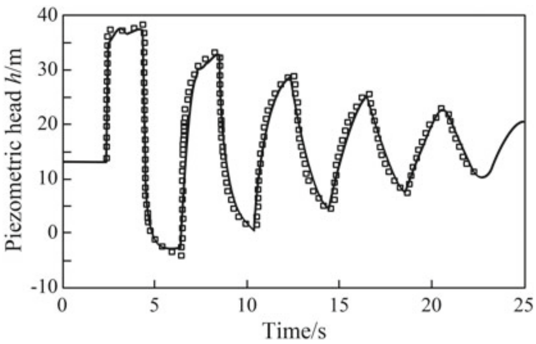

Fig. 2.9 A comparison of theoretical (*squares*) and experimental (*solid line*) wave propagation of water hammer. From Xuan et al. (2012)

In practical hydraulic systems the ratio of pipe radius to the length is typically of $O(10^{-4})$ or smaller, so one had long been satisfied with one-dimensional linearized transient flow model. The wall friction must have accumulated effect on the p-wave during a multi-period time interval, which in that model can only be added empirically. But all efforts within such a model failed to capture the strength, period, and peculiar wave pattern of the water hammer. What had been missing in such models is the *closed-loop coupling* between the compressing and shearing processes, by which the strong pressure wave generates strong vorticity wave at pipe wall via (2.3.7), known as Stokes wave (for details see Sects. 4.1.3 and 4.3), and the latter in turn strongly modulates the former. To capture this key physics one has to consider at least a viscous axisymmetric transient flow model with coupled equations for axial and radial velocities. The problem can then be reduced to a linear integral-differential equation for p, of which an almost-analytic solution was found by Xuan et al. (2012). Remarkably, a simple enlargement of the constant molecular viscosity already enables predicting turbulent water hammer in excellent agreement with experiments, see Fig. 2.9. The theory has also led to a very effective water-hammer control principle physically.

Example 2: Flow instability in combustion chamber. If in the above example the ratio of pipe radius to length is not small, the transient flow can no longer be linearized. Internal self-nonlinearities of three processes and their nonlinear coupling as well as linear boundary coupling will all occur. This transient flow may happen in a rocket combustor, where combustion instability may trigger strong pressure waves propagating back and forth in the combustion chamber, which "rub" vorticity waves at chamber wall that in turn modulate the pressure waves. The closed-loop interactions of the processes may reach a resonance that could damage the combustor. A successful predictive theory has been developed by Flandro et al. (2006), which includes all major interactions. Figure 2.10 compares the measured and predicted time history of pressure wave in a model combustion chamber. The highly nonlinear feature of the p-wave, including the sudden increment of mean pressure (DC shift), is captured by the theory.

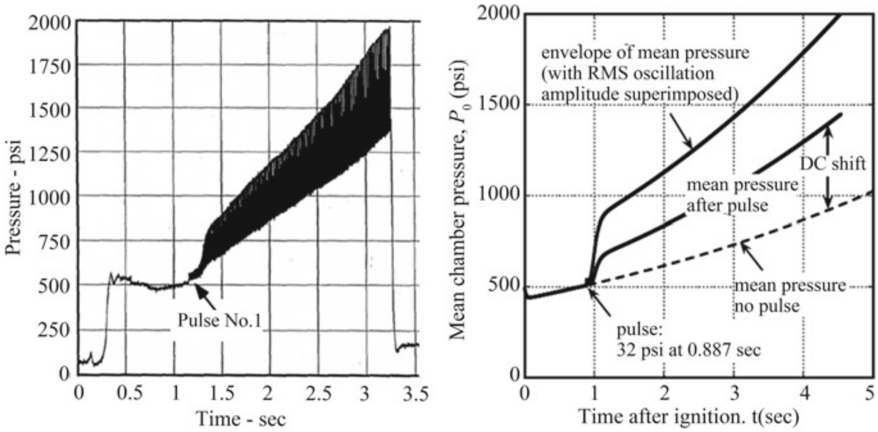

Fig. 2.10 Measured (*left*) and predicted (*right*) pressure history in a model combustion chamber. From Flandro et al. (2006)

2.3.3 Linearized Process Splitting in Unbounded Space

Having discussed how the fundamental processes in fluid motion are coupled, in what situation they can be fully split is also evident: If our concern is confined to unbounded flow, then the boundary coupling of fundamental processes of fluid motion disappears; and if the processes are just quite small disturbances of magnitudes of $O(\epsilon) \ll 1$ to a uniform flow field so that their governing equations can be linearized, then their nonlinear coupling can also be neglected. This linearized case, although simple but of fundamental significance, has been addressed by Wu (1956) and revisited by Mao (2010).

Consider a linearized viscous and heat-conducting fluid motion of arbitrary Reynolds number and Mach number, on a uniform flow background denoted by suffix ∞. Define the disturbed quantities by

$$
\begin{aligned}
&\boldsymbol{u} = U_0(\epsilon \boldsymbol{u}' + \cdots), \quad \rho = \rho_\infty(1 + \epsilon\rho' + \cdots), \quad h = c_p T_\infty(1 + \epsilon h' + \cdots),\\
&s = c_p(\epsilon s' + \cdots), \quad \nu = \nu_\infty(1 + \epsilon\nu' + \cdots),\\
&\nu_\theta = \nu_{\theta\infty}(1 + \epsilon\nu' + \cdots), \quad k = k_\infty(1 + \epsilon k' + \cdots),
\end{aligned}
$$

along with $(\vartheta, |\boldsymbol{\omega}|) = O(\epsilon)$. The prime disturbance variables are dimensionless. Then to the order of $O(\epsilon)$, (2.2.15) and (2.2.17) are reduced to a pair of linear equations

$$(\partial_t - \nu_\infty \nabla^2)\boldsymbol{\omega} = \mathbf{0}, \tag{2.3.8a}$$

$$(\partial_t^2 - a_\infty^2 \nabla^2)\vartheta = \nu_{\theta\infty}\nabla^2\partial_t\vartheta - \epsilon a_\infty^2 \nabla^2 \partial_t s'. \tag{2.3.8b}$$

Evidently, the transverse and longitudinal processes, associated with velocities $\boldsymbol{v}$ and $\nabla\phi$, respectively, are decoupled. It can be easily shown that the splitting $\boldsymbol{u} = \boldsymbol{v} + \nabla\phi$ is unique if the initial values of $\boldsymbol{v}$ and $\nabla\phi$ are given.

Then, to transform the entropy term in (2.3.8b), we use the linearized version of entropy equations (1.2.31c) and (2.2.16), now written as:

$$\partial_t s' = \frac{\gamma - 1}{\gamma a_\infty^2} \kappa \nabla^2 h',$$
$$(\partial_t - \nu_\theta \nabla^2)\vartheta = \epsilon(-\nabla^2 h' + h_\infty \nabla^2 s'),$$

where $\kappa \equiv \gamma\nu_\infty/Pr$ is known as the *thermometric conductivity*. Combining these equations yields

$$\frac{(\gamma - 1)\kappa}{\gamma a_\infty^2} \partial_t \vartheta = -\epsilon \left(\partial_t - \frac{\kappa}{\gamma}\nabla^2\right) s'.$$

We further assume that the viscosity and heat conductivity are small:

$$\epsilon \ll \nu, \nu_\theta, k = O(\delta) \ll 1. \tag{2.3.9}$$

In this case, observe that s' is of also $O(\delta)$, smaller than other variables, and hence $\kappa/\gamma\nabla^2 s' = O(\delta^2)$ should be neglected. Therefore, substituting the above ϑ-s relation into (2.3.8b) simplifies the latter to

$$(\partial_t^2 - a_\infty^2 \nabla^2) f = b\nabla^2 \partial_t f, \quad b \equiv \kappa - \frac{\kappa}{\gamma} + \nu_{\theta\infty}, \tag{2.3.10}$$

where f can stand for ϕ, ϑ, or p. The entropy also satisfies (2.3.10) if terms of both $O(\epsilon\delta)$ (its leading order) and $O(\epsilon\delta^2)$ are retained. Thus, the longitudinal process has been further split to independent compressing process and entropy process. Note that while (2.3.8a) is a standard *parabolic* (diffusion) equation (2.3.10) is a third-order parabolic equation that will degenerate to the standard hyperbolic wave equation if $b = 0$ as it should. Since the dissipation has been neglected as a nonlinear effect, the role of viscosity-conductivity in (2.3.10) is to make the longitudinal waves *dispersive* that are eventually flattened.

The above results can be stated as (Wu 1956; Mao et al. 2010).

Linear Splitting Theorem. *In an unbounded domain where the fluid is otherwise at rest, a linearized viscous and heat-conducting disturbance flow* $(\mathbf{u}, p, s)$ *may be expressed as the sum of a transverse (shearing) process and a longitudinal process governed by parabolic equations* (2.3.8a) *and* (2.3.8b)*, respectively, and* $\mathbf{u} = \mathbf{v} + \nabla\phi$*. This splitting is unique if the initial values of* $\mathbf{v}$ *and* $\nabla\phi$ *are given. Moreover, for small viscosity and heat conductivity given by* (2.3.9)*, the longitudinal process can be further decoupled to "sound mode" and "entropy mode", both governed by* (2.3.10).

We remark that the solutions of the above linear equations can also be superposed to a known basic flow field to study how the latter affects the propagation of linear viscous vortical, acoustic, and entropy waves. In this case the basic flow can be symbolically treated as the sources of mass, external body force, and heat addition, which makes (2.3.8a) and (2.3.8b) or (2.3.10) inhomogeneous as given by Mao et al. (2010).

2.4 Far-Field Asymptotics in Unbounded Flow

A fundamental issue in all studies of externally unbounded flows is the asymptotic behavior of vorticity and dilatation field as $r \equiv |\boldsymbol{x}| \to \infty$. This is a necessary prerequisite for not only prescribing far-field boundary conditions for external-flow problems, but also ensuring the convergence of relevant integrals of $\boldsymbol{\omega}$ and ϑ, including their "induced" velocity field, over the entire space or arbitrarily large external boundary. Having developed the general theory of process splitting and coupling, we can now address this issue in more detail than the velocity condition at infinity mentioned briefly in Sect. 1.3.1.

Throughout this book, whenever the fluid is externally unbounded, we start from an infinitely extended space (free space) V_∞ with fluid at rest and having uniform properties at infinity:

$$\boldsymbol{u} = \boldsymbol{0}, \quad (\boldsymbol{\omega}, \vartheta) = (\boldsymbol{0}, 0), \quad (p, \rho, s) = (p_\infty, \rho_\infty, s_\infty) \quad \text{at} \quad r \equiv |\boldsymbol{x}| = \infty. \tag{2.4.1}$$

We assume that the flow is created by a moving body (bodies) of finite size. The dynamics of the flow is Galilean invariant, and we may superimpose a constant velocity $\boldsymbol{U}$ to $\boldsymbol{u}$, with the understanding that (2.4.1) holds for the disturbance part of the composite velocity field $\boldsymbol{u} + \boldsymbol{U}$.

2.4.1 Vorticity and Dilatation Far Fields

No matter how strong, nonlinear, and coupled can various dynamic processes be in a volume $V_{NL} = O(L^n)$ around the body, with n being spatial dimension, (2.4.1) requires all disturbances to die out at infinity. Hence, there must be a far-field region V_L between V_{NL} and infinity where all processes have decayed to a weak level of $O(\epsilon) \ll 1$ and satisfy *linearized equations* derived in Sect. 2.3.3. This permits us to determine the far-field behaviors of $\boldsymbol{\omega}$ and ϑ separately.

Before proceed, we make a few general observations. Firstly, conventionally the asymptotics of parabolic equations is referred to as the state $t \to \infty$. This limiting approach cannot be used here, since it would lead to a far field contradicting (2.4.1). Instead, we should require finite $t < \infty$ but allow $r \to \infty$. For example, when a wing starts to move at $t = 0$, as will be explained in the next chapter, its generated vortex system forms a closed loop, of which the streamwise extension, say $L(t)$, is continuously elongated as t. Thus for studying the far-field behavior of the vortex loop the flow domain has to be correspondingly expanded. As long as $t < \infty$, there always exists a sufficiently large sphere of radius $r_0 \gg L(t)$ such that for $r \gg r_0$ the loop still looks like a small vortex ring near the origin.

Secondly, as is familiar in heat equation, a parabolic wave generated at $t = 0$ can propagate instantly to infinity but decays *exponentially* as distance. The former property implies that physically parabolic equations do not describe deterministic phenomena but are a statistic model for disturbances propagated by molecules, since there is no upper bound on the possible velocities of the molecules. The latter property implies that a parabolic field can never be mathematically compact with a finite support outside which the field is exactly zero. However, there always exists a finite domain outside which the parabolic field is exponentially small and hence negligible. Throughout the book we shall use the word "*compact*" in this ordinary sense, despite mathematically the field is still not strictly compact.

Thirdly, for a remote observer at $r = |\boldsymbol{x}| \gg L$, the body or even the whole region V_{NL} may be viewed as a point-like disturbance to the fluid at the origin $r = 0$. Moreover, to satisfy the upstream and downstream conditions, the disturbance cannot be of step-function type but has to be of doublet type, namely a *pulse signal*, which is of course a compact disturbance. The body motion can only reach a finite distance for any $t < \infty$, and as $r \to \infty$ this motion appears increasingly slow as if we look at a remote airplane. Thus, the flow in n-dimensional space can well be assumed symmetric with respect to x for $n = 1$, axisymmetric for $n = 2$, and spherically symmetric for $n = 3$. Consequently, it suffices to estimate the asymptotic behaviors of $(\boldsymbol{\omega}, \vartheta)$-field by using the symmetric fundamental solutions of (2.3.8a) and (2.3.10), with r being the only spatial variable. For $n = 1$, 2, and 3, r represents rectangular coordinator $|x|$, polar radius, and radius, respectively.

The above observations can be demonstrated by the fundamental solutions of (2.3.8a) and (2.3.10). We drop the suffix ∞ of the reference values for neatness. First, as a standard heat equation, (2.3.8a) has fundamental solution G_n of unified form for $n = 1, 2, 3$:

$$G_n(\boldsymbol{x}, t; \boldsymbol{x}', t') = \frac{H(\tau)}{(4\pi\nu\tau)^{n/2}} \exp\left(-\frac{r^2}{4\nu\tau}\right), \tag{2.4.2}$$

where $\tau = t - t'$ and $H(\tau)$ is the Heaviside step function. Therefore, for any $t < \infty$ the vorticity field must decay exponentially like e^{-r^2} as $r \to \infty$.

Similar to (2.4.2), the longitudinal wave decays faster algebraically as n increases. Thus it suffices to consider the solution of (2.3.10) with $n = 1$ for velocity $u(r, t)$, say:

$$u_{tt} - a^2 u_{xx} = b u_{xxt}.$$

The pulse signal has initial condition

$$\begin{aligned} u(0, t) &= 0 \quad \text{for } \ t < 0 \text{ and } t > \delta, \\ u(0, t) &= \frac{u_0}{\delta} \quad \text{for } \ t \in [0, \delta], \ \ \delta \to 0. \end{aligned}$$

The solution cannot be expressed in closed form, but its asymptotic behavior is clear. An outgoing pulse signal evolves as (the detailed algebra is skipped)

$$|\boldsymbol{u}(r,t)| = O\left(\frac{e^{-\beta r}}{r^{n/2}}\right), \quad r \to \infty, \quad t < \infty, \tag{2.4.3}$$

where β is a positive constant, which decays also exponentially but slower than vorticity. The estimate of ϑ is the same as (2.4.3). Therefore, we may state (Liu et al. 2014)

Vorticity-Dilatation Compactness. *In an unbounded compressible fluid at rest at infinity in* n*-dimensional space with* $n = 2, 3$, *originally compact vorticity and dilatation fields must remain compact in a sufficiently large domain for any finite* $t < \infty$.

The compactness of the vorticity and dilatation field ensures the finiteness of their mth tensorial moment integrals over the space for finite integers m:

$$\left\|\int_{V_\infty} \boldsymbol{xx}\ldots\boldsymbol{x}\boldsymbol{\omega} dV\right\| < \infty, \quad \left\|\int_{V_\infty} \boldsymbol{xx}\ldots\boldsymbol{x}\vartheta dV\right\| < \infty. \tag{2.4.4}$$

Owing to this *physical* compactness, the flow field in a neighborhood of infinity can only be irrotational and incompressible, which we shall always assume to have *single-valued and smooth* velocity potential.

2.4.2 Velocity Far Field

The preceding dynamic analysis of the $(\boldsymbol{\omega}, \vartheta)$ far field enables us to determine the far-field velocity induced by vorticity and dilatation through a kinematic analysis.

In addition, the assumed boundary condition (2.4.1) at infinity ensures that for any $t < \infty$ there is:

$$\int_{V_\infty} \vartheta dV = \int_{\partial V_\infty} \boldsymbol{n}\cdot\boldsymbol{u} dS = 0, \tag{2.4.5a}$$

$$\int_{V_\infty} \boldsymbol{\omega} dV = \int_{\partial V_\infty} \boldsymbol{n}\times\boldsymbol{u} dS = \boldsymbol{0}. \tag{2.4.5b}$$

Specifically, one may conceive ∂V_∞ as the boundary of the complementary fluid volume V_{out} exterior to V_∞ and including infinity, in which as we assumed the flow has smooth and single-valued velocity potential with $\vartheta = 0$. Then (2.4.5a) follows. On the other hand, (2.4.5b) comes from a pair of general results of vorticity kinematics to be addressed in Sect. 3.3.1 below: the *Föppl total-vorticity theorem* if the spatial dimension of V_∞ is $n = 3$, and the *total-circulation theorem* if $n = 2$, both being the direct corollaries of the vorticity compactness.

Then, as seen in Sect. 2.2.1, the velocity decomposition (2.2.5) leads to Poisson equations for the scalar potential ϕ and vector potential $\boldsymbol{\psi}$ of velocity:

$$\nabla^2\phi = \vartheta, \tag{2.4.6a}$$
$$\nabla^2\boldsymbol{\psi} = -\boldsymbol{\omega}, \quad \nabla\cdot\boldsymbol{\psi} = 0, \tag{2.4.6b}$$

so that for a given $(\vartheta, \boldsymbol{\omega})$ distribution in an unbounded flow, one can solve the $(\phi, \boldsymbol{\psi})$ field as (Appendix A.3)

$$\phi = \int_{V_\infty} G\vartheta' dV', \quad \boldsymbol{\psi} = -\int_{V_\infty} G\boldsymbol{\omega}' dV', \tag{2.4.7}$$

where the two-point function $G(\boldsymbol{x}, \boldsymbol{x}')$ is the fundamental solution of the Poisson equation, representing the field at $\boldsymbol{x}$ generated by a pointwise disturbance of unit strength at $\boldsymbol{x}'$ (Fig. 2.11):

$$G(\boldsymbol{r}) = \begin{cases} \dfrac{1}{2\pi}\log r & \text{if } n = 2, \\ -\dfrac{1}{4\pi r} & \text{if } n = 3, \end{cases} \tag{2.4.8}$$

with $r = |\boldsymbol{r}|$ and $\boldsymbol{r} = \boldsymbol{x} - \boldsymbol{x}'$.

Now, while $\boldsymbol{x}'$ runs over a compact domain of $\vartheta \neq 0$ and $\boldsymbol{\omega} \neq \boldsymbol{0}$, the field point $\boldsymbol{x}$ can approach infinity with $x = |\boldsymbol{x}| \to \infty$. When $x > x' = |\boldsymbol{x}'|$, the Taylor expansion of G around $\boldsymbol{x}' = \boldsymbol{0}$ converges:

$$G(\boldsymbol{x} - \boldsymbol{x}') = G_0 - x_i'(G_{,i})_0 + \frac{1}{2}x_i'x_j'(G_{,ij})_0 - \cdots, \tag{2.4.9}$$

where the suffix 0 denotes evaluation at $\boldsymbol{x} = \boldsymbol{0}$, making the functions dependent on $\boldsymbol{x}$ only. Owing to (2.4.5), as we substitute $G(r)$ into (2.4.7) the first term has no contribution and the leading-order approximation comes from the second term depending linearly on $\boldsymbol{x}'$. Thus, let

$$\boldsymbol{I}_\theta \equiv \int \boldsymbol{x}'\vartheta' dV' \tag{2.4.10}$$

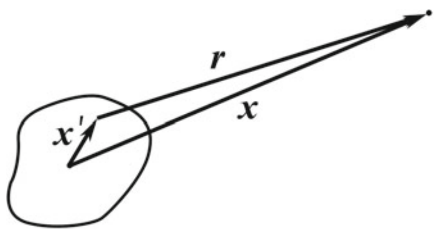

Fig. 2.11 Geometry of position vectors $\boldsymbol{x}$ and $\boldsymbol{x}'$ for observation point and field point, respectively. $\boldsymbol{r} = \boldsymbol{x} - \boldsymbol{x}'$

which by (2.4.4) must be finite, the ϑ-induced velocity has the leading-order expansion

$$\boldsymbol{u}_\theta = \nabla\phi \simeq -\nabla[\boldsymbol{I}_\theta \cdot (\nabla G)_0] = -\boldsymbol{I}_\theta \cdot (\nabla\nabla G)_0, \tag{2.4.11}$$

indicating $\boldsymbol{u}_\theta$ is irrotational as it should. It is also divergence-free, since

$$\nabla \cdot \boldsymbol{u}_\theta \simeq -I_{\theta j} G_{,jii} = 0.$$

Similarly, for the $\boldsymbol{\omega}$-induced velocity there is

$$\boldsymbol{u}_v = \nabla \times \boldsymbol{\psi} \simeq \nabla \times \int \boldsymbol{x}' \cdot (\nabla G)_0 \boldsymbol{\omega}' dV' = \nabla \times \left(\int \boldsymbol{\omega}' \boldsymbol{x}' \cdot (\nabla G)_0 dV' \right).$$

Since for $n = 3$

$$\int (\omega_i x_j + x_i \omega_j) dV = \int \nabla \cdot (x_i x_j \boldsymbol{\omega}) dV = 0, \tag{2.4.12}$$

only the anti-symmetric part of $\omega_i x_j$, i.e., $(\omega_i x_j - x_i \omega_j)/2$, has contribution to $\boldsymbol{u}_v$, namely

$$\frac{1}{2}(\boldsymbol{\omega}'\boldsymbol{x}' - \boldsymbol{x}'\boldsymbol{\omega}') \cdot (\nabla G)_0 = -\frac{1}{2}(\nabla G)_0 \times (\boldsymbol{x}' \times \boldsymbol{\omega}').$$

But (2.4.12) does not hold for $n = 2$; rather, since $\boldsymbol{\omega} = \omega \boldsymbol{e}_3$ with $\boldsymbol{\omega} \cdot \nabla G = 0$ we simply have

$$\boldsymbol{\omega}'\boldsymbol{x}' \cdot (\nabla G)_0 = -(\nabla G)_0 \times (\boldsymbol{x}' \times \boldsymbol{\omega}').$$

Hence, let

$$\boldsymbol{I}_v \equiv \frac{1}{n-1} \int \boldsymbol{x}' \times \boldsymbol{\omega}' dV' \tag{2.4.13}$$

which by (2.4.4) must also be finite, the $\boldsymbol{\omega}$-induced velocity has the leading-order expansion

$$\boldsymbol{u}_v \simeq -\nabla \times [(\nabla G)_0 \times \boldsymbol{I}_v] = -\boldsymbol{I}_v \cdot (\nabla\nabla G)_0 = -\nabla[\boldsymbol{I}_v \cdot (\nabla G)_0], \tag{2.4.14}$$

which is also irrotational as well as divergence-free.

By (2.4.8), for $n = 2$ and 3 the explicit forms of $(\nabla G)_0$ and $(\nabla\nabla G)_0$ are

$$(G_{,i})_0 = \frac{1}{2(n-1)\pi} \frac{e_i}{x^{(n-1)}}, \tag{2.4.15a}$$

$$(G_{,ij})_0 = \frac{1}{2(n-1)\pi} \frac{\delta_{ij} - n e_i e_j}{x^n}, \tag{2.4.15b}$$

where $\boldsymbol{e} = \boldsymbol{x}/x$ is the unit vector along $\boldsymbol{x}$. Therefore, we may summarize the above results as follows:

Velocity Far-Field Behavior. *In an unbounded compressible fluid at rest at infinity in n-dimensional space with* $n = 2, 3$, *if there is no net mass source nor total vorticity, then the far-field velocity induced by the vorticity and dilatation is dominated by*

$$\boldsymbol{u} = -(\boldsymbol{I}_\theta + \boldsymbol{I}_v) \cdot (\nabla\nabla G)_0 = O(x^{-n}), \tag{2.4.16}$$

which is an incompressible potential flow with $\phi = O(x^{-(n-1)})$.

2.4.3 Far-Field Asymptotics for Steady Flow

In this book, whenever we say "V extends to the entire space V_∞", we will be always talking about the "true" infinity, namely not only the fluid is at rest at infinity so that (2.4.1) is satisfied, but also V_∞ contains the whole vorticity and dilatation field so that (2.4.5a) and (2.4.5b) are satisfied. In this case the far-field flow becomes all-over irrotational so that the velocity has asymptotic behavior $|\boldsymbol{u}| = O(|\boldsymbol{x}|^{-n})$ as $\boldsymbol{x} \to \infty$ for $t < \infty$, given by (2.4.16).

Conceive now a finite body B centered at $\boldsymbol{x}_0$ starts motion in an otherwise still viscous fluid in V_∞ at $t = 0$, and then turns to move at constant velocity $\boldsymbol{U}_B = -U\boldsymbol{e}_x$. For definiteness assume the flow is incompressible. The moving body creates a disturbance flow field with nonzero vorticity. As long as the Reynolds number based on body size is not very small, the body carries a part of vorticity along with it and leaves the rest behind it, forming a *vortical wake*. The downstream end of the wake is the "starting vortical structure" generated at the earliest time $t = 0$, which stays around $\boldsymbol{x}_0$. As the body keeps moving to $x(t) = x_0 - Ut$, the wake extends from $x(t)$ to x_0, with a continuously increasing length $L(t) \sim Ut$. The flow in V_∞ is evidently time-dependent.

In the frame of reference fixed to the body, let the velocity field be $\boldsymbol{u} = \boldsymbol{U} + \boldsymbol{v}$ with $\boldsymbol{U} = -\boldsymbol{U}_B = U\boldsymbol{e}_x$, one sees

$$\boldsymbol{u} \to U\boldsymbol{e}_x \text{ and } \boldsymbol{v} \to \boldsymbol{0} \ \text{ as } |\boldsymbol{x}| \to \infty, \quad \boldsymbol{u} = \boldsymbol{0} \ \text{ for } \boldsymbol{x} \in \partial B.$$

At sufficiently large t after start, the starting vortical structure and its unsteady motion are very far away from the solid body, so their influence on the near-body flow is well negligible. Namely, the velocity field in a subspace surrounding the body, say V_{st}, may become (not always) time-independent or *steady* with $\boldsymbol{u} = \boldsymbol{u}(\boldsymbol{x})$. Meanwhile, one may set $V_\infty = V_{\text{st}} + V_{\text{nst}}$, where V_{nst} is a downstream subspace containing the starting vortical structure that retreats at speed $\boldsymbol{U}$, so the flow there is still inherently unsteady. This situation is exemplified in Fig. 2.12 for two- and three-dimensional wing flows, where the starting vortical structure is known as *starting vortex* (for details see Sects. 8.5.2 and 9.1.2).

In Fig. 2.12, the common boundary of V_{st} and V_{nst} must cut through the wake (as a *wake plane*) to exclude the unsteady growth of the wake in V_{nst}. Of course the wake plane, say W, should be located sufficiently far from the active unsteady-

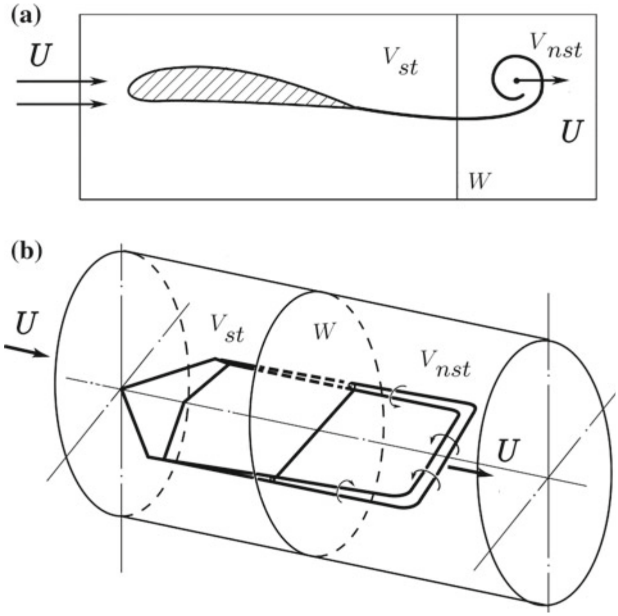

Fig. 2.12 Wing wake including starting vortex in, **a** two dimensions and **b** three dimensions. The flow in $V_{\rm st}$ is steady and that in $V_{\rm nst}$ is unsteady. The common boundary of $V_{\rm st}$ and $V_{\rm nst}$ is a wake plane W

flow region in $V_{\rm nst}$ so that at W all flow unsteadiness cannot be felt, where one can set time-independent downstream boundary conditions for the flow in $V_{\rm st}$. In $V_{\rm st}$, then, one sees an *open* wake, like an "infinitely" long paraboloid shown in Fig. 1.10. Evidently, this type of viscous steady flow must have different far-field asymptotics as $|\boldsymbol{x}| \to$ "∞". Since having two distinct infinite spaces V_∞ and $V_{\rm st}$ with different boundary conditions at infinity could tempt one to forget their inherent physical relation, we prefer to put them into a unified picture by assuming the steady flow to occur at arbitrarily large but finite t, so that $V_{\rm st}$ and $V_{\rm nst}$ are two true subset of V_∞ shown in Fig. 2.12. Therefore, the integral condition (2.4.5b) no longer holds over $V_{\rm st}$, but we now have

$$\int_{V_{\rm st}} \boldsymbol{\omega} dV = -\int_{V_{\rm nst}} \boldsymbol{\omega} dV, \quad n = 2, 3. \tag{2.4.17}$$

Namely, owing to (2.4.5b), the vortical structures in $V_{\rm st}$ and $V_{\rm nst}$ must coexist, one implying another.

Accordingly, the far-field estimate of velocity (2.4.16) in $V_{\rm st}$ has to be revised due to two distinct reasons. The first revision comes from the special property of two-dimensional flow, which also holds for unsteady flow. For any three-dimensional flow over a finite body, the flow domain $V_f = V_\infty - B$ is singly-connected and (2.4.5b) always holds. By contrast, in two dimensions V_f is *doubly-connected*. Even if $\boldsymbol{u} = \nabla\phi$ throughout $V_{\rm st}$, the potential ϕ can be multi-valued and gains an arbitrary nonzero circulation Γ along any loop surrounding the body once. Such a potential is called *cyclic* or *circulatory*. For this case (2.4.5b) and (2.4.14) are invalid in any domain enclosing the body. Instead, in the far-field Taylor expansion (2.4.9) of Green's function $G(\boldsymbol{x}-\boldsymbol{x}_0)$, the first term will be G_0 rather than $x_i'(G_{,i})_0$, with the coefficient being that Γ. Consequently, if at far field the two-dimensional flow is *irrotational*, the expansion of potential ϕ has an extra leading term:

$$\phi = \frac{\Gamma}{2\pi}\theta + c_i\partial_i(\log r) + c_{ij}\partial_i\partial_j(\log r) + \cdots ,$$

where θ is the polar angle and we have assumed no source of mass as before. Thus, for $\boldsymbol{x} \in V_{\rm st} \subset V_\infty$ and as $|\boldsymbol{x}| \to$ "∞", to the leading order there is

$$\boldsymbol{v} = \frac{\Gamma}{2\pi}\nabla\theta = \boldsymbol{e}_\theta\frac{\Gamma}{2\pi r} = O(r^{-1}). \tag{2.4.19}$$

The second and more delicate revision comes from the "infinitely" extended paraboloidal wake in viscous vortical flow, for which neither (2.4.19) nor (2.4.16) is applicable. Rather, instead of (2.3.8a), the linearized far-field vorticity equation for steady flow reads

$$\left(\nabla^2 - 2k\frac{\partial}{\partial x}\right)\boldsymbol{\omega} = \boldsymbol{0}, \quad k \equiv \frac{U}{2\nu}, \tag{2.4.20}$$

known as the *Oseen equation*, which is uniformly effective at any $Re = Ua/\nu$, where a is the body length scale. For example, for steady flow over a sphere, in spherical coordinates (r, ϕ, θ) with $x = r\cos\theta$, the vorticity $\boldsymbol{\omega} = \omega\boldsymbol{e}_\phi$ is along the azimuthal direction, and to the leading order of $a/r \ll 1$ (2.4.20) has approximate solution (e.g., Lamb 1932; Milne-Thomson 1968)

$$\omega = A(1+kr)\frac{\sin\theta}{r^2}e^{-kr(1-\cos\theta)} \quad \text{for } r \gg a, \tag{2.4.21}$$

where constant A is to be determined by the solution near the sphere at $R = O(a)$. The exponential factor in (2.4.21) describes a paraboloidal wake

$$r(1-\cos\theta) = L > 0, \quad r = |\boldsymbol{x}|,$$

outside which the vorticity decays exponentially but inside which it decays much slowly. Consequently, the far-field behavior of velocity is also different from (2.4.16). A rigorous estimate (Galdi 2011) has shown that outside the wake only the transverse components of $\boldsymbol{u}(\boldsymbol{x})$ decay according to (2.4.16) for $n = 3$ or $n = 2$ with $\Gamma = 0$, or (2.4.19) for $n = 2$ with $\Gamma \neq 0$; while for $\boldsymbol{v}\cdot\boldsymbol{e}_x = v_x(\boldsymbol{x})$ there is

$$|v_x(\boldsymbol{x})| = O(r^{-1/2}) \quad \text{as} \quad r \to \text{“}\infty\text{”}, \quad \boldsymbol{x} \in \text{wake}, \tag{2.4.22a}$$

$$|v_x(\boldsymbol{x})| = O(r^{-1/2-\epsilon}) \quad \text{as} \quad r \to \text{“}\infty\text{”}, \quad \boldsymbol{x} \notin \text{wake}, \tag{2.4.22b}$$

for some $\epsilon > 0$.

2.5 A Decoupled Model Flow: Inviscid Gas Dynamics

Owing to the big difficulty in theoretical studies of general viscous and compressible flows with coupled shearing and compressing processes, various simplified flow models have been developed and extensively explored to minimize the process coupling. The basis of these models is the fact that the behavior of shearing and compressing processes are governed by the Reynolds number Re and Mach number M, respectively, and hence their decoupling is possible if one of these numbers becomes infinity or zero. Two most widely used model flows are thereby identified: inviscid gas dynamics with $Re \to \infty$, which is briefly reviewed in this section; and viscous incompressible flow with $M \to 0$, which is the subject of the next section.

2.5.1 Basic Equations

We have seen in Sect. 1.2.4 that, for flow over a streamlined body at large Reynolds number Re, the shearing process is confined in a very thin *boundary layer* and its wake, outside which the global flow can be treated as effectively inviscid and irrotational. Therefore, one can consider the *asymptotic flow model at* $Re \to \infty$, neglect the thickness of the boundary layer, assume that the global flow satisfies only the no-through condition (1.3.2a) at the body surface. Then the linear viscous boundary coupling between the compressing and shearing processes disappears, and one can solve the inviscid global flow field first by the following equations:

$$\frac{D\rho}{Dt} + \rho\vartheta = 0, \tag{2.5.1a}$$

$$\rho\frac{D\boldsymbol{u}}{Dt} = -\nabla p, \tag{2.5.1b}$$

$$\rho T\frac{Ds}{Dt} = 0, \tag{2.5.1c}$$

$$p = \rho R T. \tag{2.5.1d}$$

The Euler equation (2.5.1b) can be replaced by the *Crocco equation* (2.2.11) for per unit mass:

$$\frac{\partial \boldsymbol{u}}{\partial t} + \boldsymbol{\omega} \times \boldsymbol{u} = -\nabla H + T\nabla s. \tag{2.5.2}$$

On the other hand, it is often convenient to replace (2.5.1c) by the total-enthalpy equation (1.2.34), which now reads

$$\rho \frac{DH}{Dt} = \frac{\partial p}{\partial t}. \tag{2.5.3}$$

These equations form the basis of *inviscid gas dynamics theory*, e.g., Liepmann and Roshko (1957). The no-slip condition (1.3.2b) will be imposed only when the viscous shear flow in boundary layer is to be solved for calculating the skin friction. This ingenious strategy invented by Prandtl in 1904 has been proved to be extremely successful and applied widely in practice.

2.5.2 Unsteady Potential Flows

If the flow remains attached and curved shock-waves therein, if any, are weak so that the entropy gradient behind the shocks is small, the flow away from boundary can be further treated irrotational with $\boldsymbol{u} = \nabla\phi$,[7] so that one obtains a fully decoupled model flow in which only one- two-, or three-dimensional longitudinal (compressing and entropy) process exists, with $Ds/Dt = 0$ following fluid particles' motion except across shock waves. This *isentropic* condition can be further strengthened to *homoentropic* condition $s = s_\infty$ if in far upstream the flow is uniform with constant s_∞. Then for arbitrary inviscid fluid (2.5.2) is reduced to

$$\nabla\left(\frac{\partial\phi}{\partial t} + H\right) = 0,$$

which can be integrated once to yield the unsteady Bernoulli equation

$$\frac{\partial\phi}{\partial t} + h + \frac{1}{2}|\nabla\phi|^2 = \frac{\partial\phi}{\partial t} + \int\frac{dp}{\rho} + \frac{1}{2}|\nabla\phi|^2 = 0, \tag{2.5.4}$$

where the integration constant $C(t)$ has been absorbed into ϕ without loss of generality. Then, by (2.5.1a), (2.5.1c), and thermodynamic relation (1.2.26), (2.5.4) is cast to

$$\nabla^2\phi = -\frac{1}{\rho}\frac{D\rho}{Dt} = -\frac{1}{a^2}\frac{Dh}{Dt} = \frac{1}{a^2}\frac{D}{Dt}\left(\frac{\partial\phi}{\partial t} + \frac{1}{2}|\nabla\phi|^2\right),$$

in which $D/Dt = \partial_t + \nabla\phi\cdot\nabla$. Hence, we obtain the *unsteady velocity potential equation* for homoentropic flow of any fluid:

$$\frac{\partial^2\phi}{\partial t^2} + \frac{\partial}{\partial t}|\nabla\phi|^2 + \nabla\phi\cdot\nabla\nabla\phi\cdot\nabla\phi - a^2\nabla^2\phi = 0; \tag{2.5.6a}$$

[7] If a shock is strong, the curl of (2.5.2) indicates that $\nabla T \times \nabla s$ will produce vorticity, see Sect. 3.4.2.

or, in more compact form,

$$\frac{D^2\phi}{Dt^2} - \frac{D}{Dt}\left(\frac{1}{2}|\nabla\phi|^2\right) - a^2\nabla^2\phi = 0. \tag{2.5.6b}$$

These equations are the basis of *nonlinear acoustics theory*.

2.5.3 Steady Isentropic Flow

Consider now a uniform incoming flow $\boldsymbol{U}$ over a stationary body, where the inviscid flow can often be treated steady. Then it is easily seen that (2.2.17) can be integrated twice and reduced to the first-order nonlinear *velocity equation* for inviscid isentropic flow, well known in gas dynamics (Problem 2.1):

$$\boldsymbol{u}\cdot\mathbf{D}\cdot\boldsymbol{u} - a^2\nabla\cdot\boldsymbol{u} = 0, \quad \text{or} \tag{2.5.7a}$$

$$\boldsymbol{u}\cdot\nabla\left(\frac{1}{2}q^2\right) - a^2\nabla\cdot\boldsymbol{u} = 0, \tag{2.5.7b}$$

where $\mathbf{D}$ is the symmetric strain-rate tensor. This equation is the first of two basic equations for inviscid, isentropic, and steady flow. To see its component form, it suffices to consider two-dimensional flow on (x, y)-plane with $\boldsymbol{u} = (u, v)$. Denote partial derivatives by subscripts, (2.5.7) yields

$$\left(1 - \frac{u^2}{a^2}\right)u_x + \left(1 - \frac{v^2}{a^2}\right)v_y - \frac{uv}{a^2}\left(v_x + u_y\right) = 0. \tag{2.5.8}$$

Obviously, the velocity equation will be most useful if $\boldsymbol{u}$ can be expressed in terms of a single scalar variable, e.g. by ϕ for potential flow or by ψ for two-dimensional flow. Then (2.5.7) or (2.5.8) becomes an equation for that scalar alone. For example, in terms of ϕ, (2.5.8) becomes the second-order *full velocity-potential equation* (cf. Problem 2.6).

Equation (2.5.7) alone is not yet closed as it involves variable sound speed a. This variable comes from the total-enthalpy equation (2.5.3) that simply reads $\boldsymbol{u}\cdot\nabla H = 0$, yielding the *energy integral*

$$H = \frac{1}{2}q^2 + h = \frac{1}{2}q^2 + c_pT = C(\psi), \tag{2.5.9a}$$

where ψ is a symbolic notation of a streamline. For polytropic gas this equation is specified to

$$\frac{1}{2}q^2 + \frac{\gamma}{\gamma-1}\frac{p}{\rho} = \frac{1}{2}q^2 + \frac{a^2}{\gamma-1} = C(\psi), \tag{2.5.9b}$$

or

$$a^2 = a_\infty^2 + \frac{\gamma - 1}{2}(U^2 - q^2), \tag{2.5.10}$$

which is the second of two basic equations for inviscid, isentropic, and steady flow. Equations (2.5.7) and (2.5.10) constitute the very basis of *high-speed steady aerodynamics* from subsonic to supersonic flows (for supersonic flow the jump relations across shock waves need to be added). This subject is beyond the concern of the present book (but see Problems 2.6 and 2.7).

2.6 Minimally-Coupled Model: Incompressible Flow

Alternative to the above asymptotic model with $Re \to \infty$, the asymptotic model with $M \to 0$ leads to *viscous incompressible flow* with $\vartheta = \nabla \cdot \boldsymbol{u} = 0$, in which the compressing-shearing coupling is minimized. In practice one does not require this velocity solenoidality condition to hold exactly, but will consider the flow as incompressible if the following dimensionless numbers are all small (Lighthill 1963):

$$\frac{nL}{a_\infty}, \frac{U}{a_\infty}, \frac{T_w - T_\infty}{T_\infty}, \frac{gL}{a_\infty^2} \ll 1, \tag{2.6.1}$$

where n is characteristic frequency, T_w the wall temperature, g the gravitational acceleration. These conditions can be inferred from inspecting (1.2.41c) and (1.2.44). Then thermodynamics is not involved either. Note that while (1.2.41a) and (1.2.44) suggest that the compressibility effect is proportional to M_∞^2, very high-frequency density fluctuation may result in $\vartheta \neq 0$ and this effect is proportional to M_∞. Indeed, comparing the Strouhal number St_a based on a_∞ as in (2.6.1) and that based on U yields $St_a/St = M_\infty$. Obviously, the incompressible flow is the best simplified model for the study of vortical flows. Most contents of this book will be developed within this model. Before entering the vorticity and vortex dynamics, therefore, it is appropriate to review the general theoretical foundation of incompressible flow.

2.6.1 Momentum Formulation versus Vorticity Formulation

For incompressible flow, the compressing process is degenerated to and only represented by the mechanical pressure field p. What remain nontrivial in the general Navier-Stokes equations are only the continuity equation (which becomes a kinematic constraint) and momentum equation, sufficient for solving $\boldsymbol{u}$ and p:

$$\nabla \cdot \boldsymbol{u} = 0, \tag{2.6.2a}$$

$$\begin{aligned} \rho \frac{D\boldsymbol{u}}{Dt} &= -\nabla p + \mu \nabla^2 \boldsymbol{u} \\ &= -\nabla p - \mu \nabla \times \boldsymbol{\omega}. \end{aligned} \tag{2.6.2b}$$

Alternative to (2.6.2b), we may write

$$\frac{\partial \boldsymbol{u}}{\partial t} + \boldsymbol{\omega} \times \boldsymbol{u} = -\nabla H - \nu \nabla \times \boldsymbol{\omega} \tag{2.6.3}$$

for per unit mass, where $H = p/\rho + q^2/2$.

For flow over a solid boundary, it is well known that (2.6.2) and velocity adherence condition (1.3.2),

$$[\![\boldsymbol{u}]\!] = \boldsymbol{0} \quad \text{at boundary}, \tag{2.6.4}$$

along with external flow condition, form a well-posed problem, which we call *momentum formulation*. But due to the $(\boldsymbol{u}, p)$ coupling inside the fluid, pressure has also to be solved, from the divergence of (2.6.2b) or (2.6.3):

$$\nabla^2 p = -\rho \nabla \cdot (\boldsymbol{u} \cdot \nabla \boldsymbol{u}) = -\rho \nabla \boldsymbol{u} : \nabla \boldsymbol{u}, \tag{2.6.5a}$$

$$\nabla^2 H = -\nabla \cdot (\boldsymbol{\omega} \times \boldsymbol{u}). \tag{2.6.5b}$$

These Poisson equations indicate that p and H are variables depending on the entire instantaneous flow field with no progressing wave.

Actually, since all flow structures of incompressible flow come solely from the shearing process, pressure behavior in the interior of a flow is not our concern. It can be removed by taking the curl of (2.6.2b) or (2.6.3) (assuming no non-conservative external body force):

$$\frac{\partial \boldsymbol{\omega}}{\partial t} + \nabla \times (\boldsymbol{\omega} \times \boldsymbol{u}) = \frac{D\boldsymbol{\omega}}{Dt} - \boldsymbol{\omega} \cdot \nabla \boldsymbol{u} = \nu \nabla^2 \boldsymbol{\omega}, \tag{2.6.6}$$

which is known as the *Helmholtz vorticity equation*. In the interior of the flow the shearing has only a self-nonlinearity. In contrast to (2.6.5), this equation involves *time evolution* and *viscous diffusion* of vorticity. In fact, one could well calculate the $(\boldsymbol{u}, \boldsymbol{\omega})$-field first by solving (2.6.6) along with $\boldsymbol{\omega} = \nabla \times \boldsymbol{u}$, of which the inversion is the Biot-Savart formula to be addressed in the next chapter, and then calculate pressure p.

Under the velocity adherence condition (2.6.4), however, unlike (2.6.2b), (2.6.6) *does not* form a well-posed problem because it is one order higher than (2.6.2b) and possible spurious solution could appear. The same is true for (2.6.5). Additional boundary conditions are necessary, of which the natural (and optimal) choice is *dynamic boundary conditions of Neumann type*, derived from (2.6.2b) itself applied on boundary with the use of acceleration adherence (1.3.3).

For example, consider two-dimensional flow on the (x, y) plane over a wall with $\boldsymbol{u} = (u, v)$, $\boldsymbol{\omega} = \boldsymbol{e}_z\omega$, and acceleration $\boldsymbol{a}_B = (a_{sB}, a_{nB})$. In this case (2.6.6) degenerates to

$$\frac{D\omega}{Dt} = \nu\nabla^2\omega, \tag{2.6.7}$$

and the additional conditions for vorticity and pressure are a simple extensions of (2.3.7a) and (2.3.7b), respectively:

$$\nu\frac{\partial\omega}{\partial n} = \frac{1}{\rho}\frac{\partial p}{\partial s} + a_{sB}, \tag{2.6.8a}$$

$$\frac{1}{\rho}\frac{\partial p}{\partial n} = -\nu\frac{\partial\omega}{\partial s} - a_{nB}. \tag{2.6.8b}$$

As remarked in Sect. 1.3.1, as long as (2.6.4) holds at $t = 0$, it is ensured by (2.6.8a). We thus call (2.6.7) and (2.6.8a), as well as their extension to three dimensions, the *vorticity formulation*. The interior $(\boldsymbol{u}, p)$ coupling becomes a viscous (ω, p) coupling at boundary via viscosity and no-slip condition.

Vortical structures appear in flows with $Re \gg 1$ only. In this case $\omega = O(Re^{1/2})$ as will be seen in boundary layer and free shear layer (Chap. 4). Since $\partial/\partial s = O(1)$, if $Re \gg 1$ and $a_{nB} = 0$ the right-hand side of (2.6.8b) is small and so is $\partial_n p$. But the right-hand side of (2.6.8a) remains of $O(1)$, and hence so must be the left-hand side even if $Re \to \infty$. Therefore, (2.6.8a) is the key relation where, as said before, $\nu\partial\omega/\partial n \equiv \sigma$ is the *boundary vorticity flux* (BVF) that measures the vorticity creation rate at the wall and diffuses the vorticity into the fluid.

Mathematically and physically, the above analysis indicates that *in viscous wall-bounded flow a completely decoupling of shearing process from compressing process is impossible.* Their coupling always exists but is *minimized* in incompressible flow.

Numerically, however, the calculation of p can be bypassed by fractional-step vorticity-based methods (cf. Wu et al. 2006), where (2.6.8a) is the key condition to be satisfied, which can be implicitly imposed. This observation has motivated many studies in fluid dynamics and applied mathematics communities to design vorticity-based numerical methods, either grid-free or with grids. Besides, in two dimensions the velocity decomposition $\boldsymbol{u} = \nabla\phi + \nabla\times\boldsymbol{\psi}$ has vector potential $\boldsymbol{\psi} = (0, 0, \psi)$ and $\boldsymbol{\psi}$ is reduced to a single scalar ψ known as the *stream function*. We thus have

$$\boldsymbol{u} = \nabla\phi + \nabla\psi\times\boldsymbol{e}_z, \quad \nabla^2\phi = 0, \quad \nabla^2\psi = -\omega. \tag{2.6.9}$$

Thus, (2.6.7) may be replaced by a fourth-order equation for ψ, fully decoupled from p.

Although practice has shown that momentum-based numerical schemes are more convenient in use than vorticity-based schemes and have been the mainstream of CFD, the latter sheds deeper and unique insight to vortical-flow physics. Especially, if the flow field has been solved by whatever formulation and the distributions of $(\boldsymbol{u}, \boldsymbol{\omega}, p)$ are all available, the vorticity formulation offers a very powerful means for understanding the physics. For example, the role of pressure in the flow evolution in vorticity formulation has much clearer physical meaning than its role in momentum formulation. In particular, since (2.6.6) is homogeneous in $\boldsymbol{\omega}$, *the BVF is the only source in incompressible flow; no BVF, no vortical flows*. In contrast, the origin of vorticity in incompressible flows is hidden in momentum formulation.

2.6.2 Incompressible Potential Flow

If we take double limits, not only $M \to 0$ but also $Re \to \infty$, then we arrive at the "inviscid" and incompressible flow model, of which the real meaning is that the flow is still viscous with $\mu \neq 0$ but $\mu \to 0$. In this model the vortical regions shrink to infinitely thin "*vortex sheets*" (Chap. 5), away from which there is $\boldsymbol{u} = \nabla\phi$. Since the vortex sheets attached to solid body surface do not alter the body geometry, we may impose the no-through condition (1.3.2a) at the body surface and thereby solve the Laplace equation $\nabla^2\phi = 0$. The viscous term in (2.6.2b) automatically disappears. This is the simplest flow model in the entire fluid dynamics, yet still an inevitable part of vortical flow theory. For example the flow "induced" by a two-dimensional *point-vortex* at origin $r = 0$ is irrotational for all $r > 0$. It is also necessary for satisfying some boundary conditions. Therefore, in the rest of this section we highlight the main content of incompressible potential-flow theory.

Consider an externally unbounded fluid domain V_f which is at rest at infinity and in which a moving body B causes a single-valued and *acyclic* (or non-circulatory) velocity potential ϕ, which is solved from the kinematic problem

$$\nabla^2\phi = 0 \quad \text{in} \quad V_f, \tag{2.6.10a}$$

$$\frac{\partial\phi}{\partial n} = \boldsymbol{n}\cdot\boldsymbol{u}_B \quad \text{on} \quad \partial B, \quad \phi \to 0 \quad \text{as} \quad x = |\boldsymbol{x}| \to \infty, \tag{2.6.10b}$$

where $\boldsymbol{u}_B$ is the velocity of ∂B. In particular, in two-dimensional flow on the (x, y) plane, the scalar stream function ψ satisfies irrotational condition $\nabla^2\psi = 0$. Thus, in complex plane $Z = x + iy$ the complex velocity potential $W(Z) = \phi + i\psi$ is analytic, making the powerful analytic-function theory and conformal mapping technique applicable.

In any case, once $\phi(\boldsymbol{x})$ is solved, the pressure can be computed from the Bernoulli integral for incompressible potential flow, which is the only dynamic equation at hand:

$$\frac{\partial\phi}{\partial t} + \frac{1}{2}|\nabla\phi|^2 + \frac{p}{\rho} = 0, \tag{2.6.11}$$

where the time-dependent integration constant is again absorbed into ϕ. An important consequence of (2.6.11) is that it leads to a very simple relation between the total pressure force acting on the body surface ∂B and the rate of change of the integral of $\phi \boldsymbol{n}$ over ∂B:

$$\rho \frac{d}{dt} \int_{\partial B} \phi \boldsymbol{n} dS = - \int_{\partial B} p \boldsymbol{n} dS. \tag{2.6.12}$$

Alternative to using (2.6.11), this relation may directly follow from integrating the Euler equation $\rho(D/Dt)\nabla\phi = -\nabla p$ over the body volume B.

If a solid body B moves through a fluid at rest at infinity and causes a potential flow, since $\nabla^2\phi = 0$ and hence $\nabla\phi \cdot \nabla\phi = \nabla \cdot (\phi\nabla\phi)$, by (2.6.10b) the total kinetic energy of the flow is

$$K = \frac{\rho}{2} \int_{V_f} \nabla\phi \cdot \nabla\phi dV = \frac{\rho}{2} \int_{\partial B} \phi \frac{\partial \phi}{\partial n} dS = \frac{\rho}{2} \int_{\partial B} \phi \boldsymbol{n} \cdot \boldsymbol{u}_B dS. \tag{2.6.13}$$

Evidently, the flow has no memory of its history but completely depends on the current motion of boundary. Since $K = 0$ implies $\nabla\phi = \mathbf{0}$ everywhere, if ∂V_f is suddenly brought to rest then the entire flow stops instantaneously. Therefore, *if there is a fluid flow without moving boundary, it must be vortical or compressible, or both.*

If one adds any disturbance $\boldsymbol{u}'$ to the velocity field with kinetic energy $K' > 0$, such that $\boldsymbol{u}_1 = \nabla\phi + \boldsymbol{u}'$, and if $\boldsymbol{u}' \cdot \boldsymbol{n} = 0$ on ∂V_f, then

$$\begin{aligned} K_1 &= \frac{\rho}{2} \int_{V_f} (\nabla\phi + \boldsymbol{u}') \cdot (\nabla\phi + \boldsymbol{u}') dV \\ &= K + K' + \rho \int_{\partial V_f} \boldsymbol{n} \cdot \boldsymbol{u}' \phi dS = K + K' > K. \end{aligned} \tag{2.6.14}$$

This is the famous **Kelvin's minimum kinetic energy theorem**: *Among all incompressible flows satisfying the same normal velocity boundary condition, the potential flow has minimum kinetic energy.*

Consider now a body moving with velocity $\boldsymbol{U}(t)$ through a three dimensional fluid at rest at infinity. Alternative to (2.6.13) that expresses the total kinetic energy K by the potential at body surface, we may express K by the far-field velocity obtained in Sect. 2.4.2. In the fluid domain V_f surrounding a body of volume V_B we have identity

$$\int_{V_f} q^2 dV = \int_{V_f} U^2 dV + \int_{V_f} (\boldsymbol{u} + \boldsymbol{U}) \cdot (\boldsymbol{u} - \boldsymbol{U}) dV. \tag{2.6.15}$$

Here, let $V = V_f + V_B$ be the volume of entire space, the first term is simply $U^2(V - V_B)$, while by using $\nabla \cdot \boldsymbol{u} = 0$ the second term is cast to

$$\int_{V_f} \nabla(\phi + \boldsymbol{U} \cdot \boldsymbol{x}) \cdot (\boldsymbol{u} - \boldsymbol{U}) dV = \int_{\partial V_f} (\phi + \boldsymbol{U} \cdot \boldsymbol{x})(\boldsymbol{u} - \boldsymbol{U}) \cdot \boldsymbol{n} dS.$$

Now ∂V_f consists of body surface ∂B and external boundary Σ, say, and on the former $(\boldsymbol{u} - \boldsymbol{U}) \cdot \boldsymbol{n} = 0$ as required by (2.6.10b). Thus the surface integral is only over Σ, which can be taken as a sphere S_R of radius $R \gg 1$ with $\boldsymbol{n} = \boldsymbol{e}$. Then, by (2.4.14), at large r the flow appears to be induced by a *dipole*:

$$\phi = -\boldsymbol{A} \cdot \nabla G = -\frac{\boldsymbol{A} \cdot \boldsymbol{e}}{r^2}, \tag{2.6.16a}$$

$$\boldsymbol{u} = \nabla\phi = -(\boldsymbol{A} \cdot \nabla)\nabla G = -\frac{\boldsymbol{A} - 3(\boldsymbol{A} \cdot \boldsymbol{e})\boldsymbol{e}}{r^3}, \tag{2.6.16b}$$

where $\boldsymbol{A}$ is proportional to $\boldsymbol{I}_v$ defined by (2.4.13), which is to be determined by the specific body shape and motion via solving (2.6.10). The constant factor $1/4\pi$ in (2.4.15) has been absorbed into $\boldsymbol{A}$. Now (2.6.15) can be cast to

$$\begin{aligned}\int_V q^2 dV &= U^2 \left(\frac{4}{3}\pi R^3 - V_B\right) \\ &\quad + \int_{S_R} \left[3(\boldsymbol{A} \cdot \boldsymbol{e})(\boldsymbol{U} \cdot \boldsymbol{e}) - R^3(\boldsymbol{U} \cdot \boldsymbol{e})^2 - \frac{2(\boldsymbol{A} \cdot \boldsymbol{e})^2}{R^3}\right] d\Omega,\end{aligned}$$

where $d\Omega$ is the solid angle element. All three terms of the surface integral are of the form

$$a_i b_j \int_{S_R} e_i e_j d\Omega,$$

which amounts to an angle average over all directions. Since in spherical coordinates $\boldsymbol{e} = (e_x, e_y, e_z) = (\sin\theta\cos\phi, \sin\theta\sin\phi, \cos\theta)$ and $d\Omega = \sin\theta d\theta d\phi$, the integration yields

$$\int_{S_R} e_i e_j d\Omega = \frac{4\pi}{3}\delta_{ij}. \tag{2.6.17}$$

Thus, after neglecting the third term that vanishes as $R \to \infty$ and dropping the cancelling terms $(4/3)\pi R^3 U^2$, we finally obtain

$$K = \frac{1}{2}\rho \int_{V_f} q^2 dV = \frac{1}{2}\rho(4\pi\boldsymbol{A} \cdot U - V_B U^2), \tag{2.6.18}$$

where the second term is the kinetic energy of the virtual fluid displaced by the moving body. We see again that once the body stops ($\boldsymbol{U} = \boldsymbol{0}$) so does the fluid immediately.

2.6.3 Accelerated Body Motion and Virtual Mass

We now take a closer look at the flow caused by body's uniform motion. Since both (2.6.10a) and (2.6.10b) are linear in ϕ, this potential must depend linearly on the components of $\boldsymbol{U}$. Thus we may write

$$\phi = U_i \hat{\phi}_i, \quad \nabla^2 \hat{\phi}_i = 0 \text{ in } V_f, \quad \frac{\partial \hat{\phi}_i}{\partial n} = n_i, \quad i = 1, 2, 3, \tag{2.6.19}$$

such that each $\hat{\phi}_i$ is the velocity potential caused by the body motion with a unit velocity in the ith direction. By their boundary condition, $\hat{\phi}_i$ are only functions of the body-surface geometry and can be obtained once for all for a given shape. Correspondingly, the dipole $\boldsymbol{A}$ and total kinetic energy K of the flow must be a linear and a quadratic forms of U_i, respectively:

$$A_i = c_{ij} U_j, \quad K = \frac{1}{2} m_{ij} U_i U_j. \tag{2.6.20}$$

By (2.6.18) and (2.6.13) it follows that

$$m_{ij} = \rho(4\pi c_{ij} - V_B \delta_{ij}), \tag{2.6.21a}$$

$$c_{ij} = \frac{1}{4\pi} \left(\int_{\partial B} \hat{\phi}_i \frac{\partial \hat{\phi}_j}{\partial n} dS + V_B \delta_{ij} \right). \tag{2.6.21b}$$

Here, it can be ensured c_{ij} is a symmetric tensor, and have so is m_{ij}. Moreover, since K is related to the total fluid momentum $\boldsymbol{P}$ by $dK = \boldsymbol{U} \cdot d\boldsymbol{P}$, there also is

$$P_i = m_{ik} U_k, \quad \text{namely} \quad \boldsymbol{P} = 4\pi\rho \boldsymbol{A} - \rho V_B \boldsymbol{U}. \tag{2.6.22}$$

Therefore, the total force exerted to the body by the potential flow takes exactly the form of Newton's second law:

$$F_i = -\frac{dP_i}{dt} = -m_{ik} \frac{dU_k}{dt}. \tag{2.6.23}$$

which will be known for a given motion once m_{ik} are calculated. The matrix m_{ik} is called *added mass*, *apparent mass*, or *virtual mass* and should be added to the body's own mass when calculating its motion.

If the body has a rotation as well as uniform translation such that

$$\boldsymbol{u}_B(\boldsymbol{x}, t) = \boldsymbol{U}(t) + \boldsymbol{\Omega}(t) \times \boldsymbol{r}, \quad \boldsymbol{r} = \boldsymbol{x} - \boldsymbol{x}_0,$$

we may simply add a potential $\phi_\Omega = \Omega_k \hat{\phi}_k$, with boundary condition

$$\frac{\partial \hat{\phi}_k}{\partial n} = (\boldsymbol{r} \times \boldsymbol{n})_k, k = 4, 5, 6.$$

2.6.4 Force on a Body in Steady Flow

We now consider the force exerted on a body B in a steady flow $\boldsymbol{u} = \nabla \phi$ with uniform incoming velocity $\boldsymbol{U}$. This issue is of great importance since it leads to two far-reaching consequences that had strongly stimulated the development of the whole fluid dynamics. One is the *d'Alembert Paradox* (d'Alembert in 1768) that had excited enormous efforts over a century for filling the very basic gap between mathematical theory and practical observations, a gap that was finally resolved by Prandtl's *boundary layer theory* (Chap. 4). The other is the *Kutta-Joukowski theorem* (Kutta in 1902 and Joukowski in 1906) that laid down the first cornerstone of modern aerodynamics.[8]

In this steady and potential flow, the total force formula (1.3.6) applies. Assume the flow at a sufficiently larger fixed control surface Σ is irrotational, the pressure can be replaced by $-|\boldsymbol{u}|^2/2$ due to the Bernoulli integral (2.6.11):

$$\boldsymbol{F} = \rho \int_\Sigma \left(\frac{1}{2} |\boldsymbol{u}|^2 \boldsymbol{n} - \boldsymbol{u}\boldsymbol{u} \cdot \boldsymbol{n} \right) dS. \tag{2.6.24}$$

Let $\boldsymbol{u} = \boldsymbol{U} + \boldsymbol{v}$ with $\boldsymbol{v}$ being the disturbance velocity that approaches zero at infinity, such that

$$\begin{aligned} \frac{1}{2}|\boldsymbol{u}|^2 n_i - u_i u_j n_j &= \frac{1}{2}|\boldsymbol{v}|^2 n_i + U_j v_j n_i + \frac{1}{2}U^2 n_i \\ &\quad -v_i v_j n_j - U_i v_j n_j - v_i U_j n_j - U_i U_j n_j. \end{aligned}$$

Substitute this into (2.6.24) and notice that quadratic terms of $\boldsymbol{U}$ can be taken out of the integral to leave zero integrals $\int \boldsymbol{n} dS$ over Σ, and the term $U_i \int v_j n_j dS$ also integrates to zero due to $\nabla \cdot \boldsymbol{v} = 0$. To handle the remaining terms, let Σ be large enough so that quadratic terms of $\boldsymbol{v}$ in the integral are negligible. Thus (2.6.24) is reduced to

$$\boldsymbol{F} = \rho \boldsymbol{U} \cdot \int_\Sigma (\boldsymbol{v}\boldsymbol{n} - \boldsymbol{n}\boldsymbol{v}) dS = \rho \boldsymbol{U} \times \int_\Sigma \boldsymbol{n} \times \boldsymbol{v} dS. \tag{2.6.25}$$

Then, as Σ further retreats toward infinity, if condition (2.4.5) holds such that by (2.4.16) there is $|\boldsymbol{v}| = O(r^{-n})$ for spatial dimension $n = 2, 3$, the above integral approaches zero as $O(r^{-1})$. Therefore, we arrive at

[8]On the historical development of these crucial results see an inspirative book by Darrigol (2009).

The d'Alembert Paradox. *A body at constant translational motion through an unbounded incompressible fluid at rest at infinity will experience no force if the fluid has no net vorticity*

We have seen in Sect. 2.4.3, however, that for two-dimensional flow over a body, if there is a circulation Γ over $V = V_f + B$, the far-field velocity estimate becomes (2.4.19), indicating that the integral of $\boldsymbol{n} \times \boldsymbol{v}$ over Σ is of $O(1)$ no matter how large Σ is. Thus, by the generalized Gauss theorem there is

$$\int_{\Sigma} \boldsymbol{n} \times \boldsymbol{v} dS = \int_{V} \boldsymbol{\omega} dV = \boldsymbol{e}_z \Gamma,$$

where $V = V_f + B$, and we immediately obtain

The Kutta-Joukowski Theorem. *A two-dimensional unbounded, steady, and incompressible cyclic potential flow over a body with circulation Γ exerts a transverse force to the body*

$$\boldsymbol{F} = -\rho U \Gamma \boldsymbol{e}_y, \tag{2.6.26}$$

where $\Gamma < 0$ if $F_y > 0$. The determination of Γ will be studied in Chap. 9.

The above derivation of (2.6.26) is a simplified version of Joukowski's original one. All one needs in proving both d'Alembert paradox and Kutta-Joukowski theorem is that the flow is inviscid and steady in V, and irrotational at Σ, satisfying corresponding far-field conditions. However, this approach is not without flaw. Later in Sect. 9.1 we shall revisit this issue and show that (2.6.26) is an exact result for two-dimensional and steady viscous flow at the limit $Re \to \infty$, which in turn is a special case of a three-dimensional *vortex-force theory* that can be further generalized to finite-Re flow.

2.7 Problems for Chapter 2

2.1. For steady viscous and compressible flow in a free space, show that (2.2.17) is reduced to

$$(a^2 + \nu_\theta \boldsymbol{u} \cdot \nabla)\vartheta - \frac{1}{2}\boldsymbol{u} \cdot \nabla q^2 + \nu \boldsymbol{u} \cdot (\nabla \times \boldsymbol{\omega}) - a^2 \boldsymbol{u} \cdot \nabla s^* = 0, \tag{2.7.1}$$

where $s^* = s/c_p$. Then using this equation to derive (2.5.7).

2.2. Discuss the physical role of viscosity and heat-conductivity in the far-field asymptotic analysis of vorticity and dilatation fields. What would happen if they are set identically zero?

2.3. Give a detailed derivation of (2.3.7).

2.4. Estimate the order of magnitude of the normal pressure gradient at the wall based on (2.3.7b), and its Re-dependence. Compare the result with the order of magnitude of boundary vorticity flux.

2.5*.[9] It has been proved in Sect. 2.4 that, in an n-dimensional unbounded free space with the fluid at rest at infinity, $n = 2, 3$, as $x = |\boldsymbol{x}| \to \infty$ the pressure $p - p_\infty$ decays exponentially and the flow is asymptotically irrotational and incompressible, with $\phi = O(x^{-n+1})$. Assume ϕ is time-dependent there, so that on a big sphere S of radius R, from the Bernoulli equation with neglecting q^2 it follows that

$$-\int_S (p - p_\infty)\boldsymbol{n}dS = \rho \int_S \frac{\partial \phi}{\partial t}\boldsymbol{n}dS = O(1)$$

since S increases as $O(R^{n-1})$. But this assertion contradicts the exponential decay behavior of $p - p_\infty$. Please resolve this apparent paradox.

2.6. Consider a two-dimensional steady, inviscid, and homoentropic flow of polytropic gas. Let the uniform free-stream velocity be $\boldsymbol{U} = U\boldsymbol{e}_x$ and denote the disturbance flow by $\boldsymbol{u} = (u, v, w)$. Assume that

$$\frac{|\boldsymbol{u}|}{U} \ll 1, \quad \frac{|\boldsymbol{u}|}{a} \ll 1.$$

Expend (2.5.7) and (2.5.10) up to the second order of $|\boldsymbol{u}|/U$ and $|\boldsymbol{u}|/a$, and show that the perturbation equation for (u, v, w) reads (subscripts denote derivatives)

$$\left[1 - M_\infty^2 - (\gamma + 1)M_\infty^2 \frac{u}{U}\right] u_x + \left[1 - (\gamma - 1)M_\infty^2 \frac{u}{U}\right] v_y = M_\infty^2 \frac{v}{U}(u_y + v_x), \tag{2.7.2}$$

where $M_\infty = U/a_\infty$. Observe that in the linearized version the perturbation equation is elliptic if $M_\infty < 1$ and hyperbolic if $M_\infty > 1$.

2.7. In transonic regime there can be $|1 - M^2| \ll 1$, where $M = |\boldsymbol{u}|/a$ is the local Mach number. Show that in this case

$$1 - M^2 = 1 - M_\infty^2 - (\gamma + 1)M_\infty^2 \frac{u}{U} + \text{higher order terms}.$$

Then determine the appropriate form of transonic perturbation equation.

[9] Throughout the book, problems with asterisk are optional.

http://www.springer.com/978-3-662-47060-2

Vortical Flows
Wu, J.-Z.; Ma, H.-Y.; Zhou, M.-D.
2015, XIV, 446 p. 202 illus., Hardcover
ISBN: 978-3-662-47060-2